A Hybrid Double-Threshold Based Cooperative Spectrum Sensing over Fading Channels

Quoc-Tuan Vien, *Member, IEEE,* Huan X. Nguyen, *Senior Member, IEEE,* Ramona Trestian, *Member, IEEE,* Purav Shah, *Member, IEEE,* and Orhan Gemikonakli

***Abstract*—This paper investigates double-threshold based energy detector for cooperative spectrum sensing mechanisms in cognitive wireless radio networks. We first propose a hybrid double-threshold based energy detector (HDTED) to improve the sensing performance at secondary users (SUs) by exploiting both the local binary/energy decisions and global binary decisions feedback from the fusion centre (FC). Significantly, we derive closed-form expressions and bounds for the probabilities of missed detection and false alarm considering a practical scenario where all channel links suffer from Rayleigh fading and background noise. The derived expressions not only show the improved performance achieved with the HDTED scheme but also enable us to analyse the impacts of the number of the SUs and the fading channels on the cooperative spectrum sensing performance. Furthermore, based on the derived bounds, we propose an optimal SU selection algorithm for forwarding the local decisions to the FC, which helps reduce the number of forwarding bits for a lower-complexity signaling. Finally, numerical results are provided to demonstrate the validity of the analytical findings.**

***Index Terms*—Cognitive radio, cooperative spectrum sensing, energy detection, user selection, Rayleigh fading.**

I. Introduction

With the advance of wireless communications and the increase in the number of wireless devices, the growing scarcity of spectrum resources has emerged as a critical issue. Recently, cognitive radio (CR) has been proposed as a promising technology to improve spectrum efficiency by providing dynamic spectrum access [1], [2]. In CR networks (CRNs), spectrum holes can be opportunistically used by the secondary users (SUs) when licenced spectrum bands allocated for licenced primary users (PUs) are unused at some specific periods of time. The spectrum occupation of the PUs can be either continuously monitored at the SUs [3] or dynamically monitored using various signal detection methods [4], such as matched filter [5], wavelet [6] and covariance detection [7]. However, in hidden terminal problems, the spectrum sensing at the SUs is infeasible as they suffer from either shadowing or severe fading effects while the licenced spectrum bands are occupied by the nearby PUs.

Along with the proposal of CR technology, cooperative communications have attracted extensive investigations to improve data throughput and transmission quality by exploiting spatial diversity gains with relaying links [8]–[11]. Inspired by relaying techniques for cooperative communications [8]–[11], cooperative spectrum sensing (CSS) was proposed to help the shadowed SUs detect the PUs and also improve detection reliability at the SUs [12]–[23]. A CSS scheme can be divided into three phases [19] as follows:

i) *Sensing (SS) phase*: Every SU carries out local spectrum sensing (LSS) to determine locally the existence of the PU;
ii) *Reporting (RP) phase*: All SUs forward their local decisions to a fusion center (FC), i.e. a common receiver;
iii) *Backward (BW) phase*: The FC makes a global decision on the existence of the PU and then broadcasts this decision to all the SUs.

In [24], a double-threshold based energy detection (DTED) was proposed for the CSS to decrease the average number of sensing bits for bandwidth-limited channels at the expense of sensing performance loss due to the discard of the detected energy value between two thresholds. Various works on DTED were then carried out to improve the sensing performance, e.g. [25]–[28]. Generally, over a practical wireless medium, the CSS scheme suffers interference and noise from all the SS, RP and BW channels. However, most published work on the CSS assumes that the channels are perfect (i.e. error-free) with RP links [12] or with BW links [14], [24]–[28].

In this paper, we consider a practical CRN where all channel links are imperfect, DTED is employed at SUs for bandwidth-limited channels and the spectrum sensing is carried out in a cooperative manner with the assistance of a FC to deal with the hidden terminal problems. The main contributions in this work can be summarised as follows:

- A novel hybrid DTED (HDTED) is proposed for the CSS to improve the sensing performance of the CRNs by exploiting both local and global detection in terms of energy and binary values at each SU, while still protecting the PU from harmful interferences caused by the SUs. In the proposed scheme, each SU forwards to the FC the binary values of available spectrum based on two thresholds. Then, the FC makes a global decision by performing binary combination of all decisions and broadcasts its global binary decisions to all the SUs. Exploiting both local decision based on binary/energy values and global binary decision sent from the FC, each SU combines them to make a hybrid decision on the availability of the licenced spectrum.
- Closed-form expressions of the average false alarm prob-

Q.-T. Vien, H. X. Nguyen, R. Trestian, P. Shah, and O. Gemikonakli are with the School of Science and Technology, Middlesex University, The Burroughs, London NW4 4BT, UK.
Email: {q.vien; h.nguyen; r.trestian; p.shah; o.gemikonakli}@mdx.ac.uk.

ability (FAP)[1] and the average missed detection probability (MDP)[2] are then derived for the proposed HDTED scheme taking into account a practical scenario where all the SS, RP and BW channel links are characterised by Rayleigh flat fading channels. It is shown that a better CSS performance is achieved with the proposed HDTED scheme compared to the conventional DTED schemes[3]. Also, an improved MDP is obtained as the number of the SUs having binary local decisions increases.

- Bounds of the average FAP and MDP are derived with respect to the number of the SUs and the reliability of the links to evaluate the effects of the SS, RP and BW channels as well as the number of SUs on the CSS performance. It is shown that the increased number of the SUs causes a higher lower-bound of the average FAP. Additionally, both the average FAP and MDP are shown to be bounded as either the BW links are in the high signal-to-noise (SNR) regime or the number of the SUs is very large.
- An optimal user selection algorithm is proposed to select SUs for the RP phase instead of exploiting all the SUs having binary local decisions. Specifically, based on the derived performance bounds with a target FAP, an optimal number of the SUs is determined and the SUs having the highest local sensing performance are selected to forward their binary decisions to the FC. This accordingly results in a lower number of forwarding bits for lower complexity in the CSS with the proposed HDTED scheme.

The rest of this paper is organised as follows: Section II describes the system model of a typical CRN and discusses local spectrum sensing at SUs. Section III presents the proposed HDTED scheme. The performance analysis of the HDTED scheme is presented in Section IV where closed-form expressions and bounds for the FAP and MDP are derived and the optimal user selection algorithm is developed for RP phase. Numerical and simulation results are presented in Section V to validate the concepts. Finally, Section VI draws the main conclusions from this paper.

II. System Model and Local Spectrum Sensing

Figure 1 illustrates the system model of an CRN including a $\mathcal{PU}$ and N SUs $\{\mathcal{SU}_1,\mathcal{SU}_2,\ldots,\mathcal{SU}_N\}$. The $\mathcal{PU}$ is assumed to operate in a wide-band channel including K non-overlapping frequency bands $\{f_1, f_2, \ldots, f_K\}$. Let $\mathcal{H}_{1,k}^{(\mathcal{PU})}$ and $\mathcal{H}_{0,k}^{(\mathcal{PU})}$, $k = 1, 2, \ldots, K$, denote the hypothesis that f_k is occupied by $\mathcal{PU}$ and the hypothesis that f_k is available for $\{\mathcal{SU}_i\}$, respectively. In order to report the availability of the frequency bands in the transmission range of the $\mathcal{PU}$, let us define a spectrum indicator vector (SIV) of length K consisting of both binary and real values, where bits '0' and '1' represent the frequency band being utilised and being available, respectively, while real values represent the energy of the observed signal when no

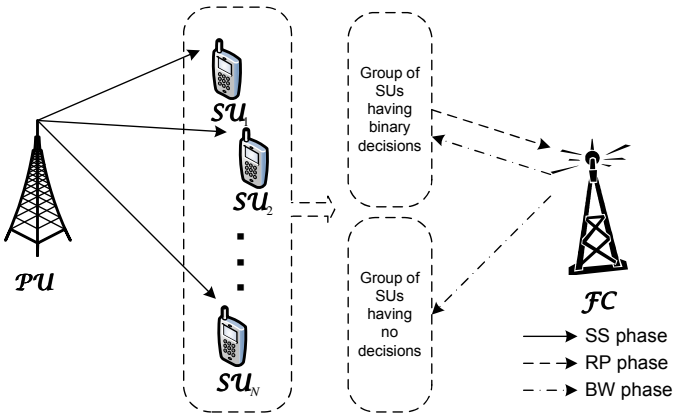

Fig. 1: System model of a cognitive radio network.

decision is made. The CSS is carried out over a common $\mathcal{FC}$. We assume that the channels for the SS links $\mathcal{PU} \rightarrow \mathcal{SU}_i$, the RP links $\mathcal{SU}_i \rightarrow \mathcal{FC}$ and the BW links $\mathcal{FC} \rightarrow \mathcal{SU}_i$, $i = 1, 2, \ldots, N$, are independent and identically distributed (i.i.d.) Rayleigh flat fading channels having channel gains of h_{PS_i}, h_{S_iF} and h_{FS_i}, respectively. A block-fading channel model is considered where all the channel gains are time-invariant over the whole transmission of both the data and the SIV, and change independently from one frame to another. In this work, noise variance is assumed to be perfectly estimated[4] and the conventional energy detection method (e.g. [24]) is applied at $\{\mathcal{SU}_i\}$.

Over the SS channel, the received signal at $\mathcal{SU}_i$ can be expressed as

$$\mathbf{r}_i^{(SS)} = h_{PS_i}\mathbf{x} + \mathbf{n}_i^{(SS)}, \tag{1}$$

where $\mathbf{x}$ is the transmitted signal vector from $\mathcal{PU}$ and $\mathbf{n}_i^{(SS)}$ is the independent circularly symmetric complex Gaussian (CSCG) noise vector at $\mathcal{SU}_i$ over the SS channel with each entry having zero mean and variance of N_0. Note that the vectors in (1) have length K which corresponds to the number of frequency bands. The elements in $\mathbf{x}$ can be equal to zero if the corresponding frequency bands are not used by the PU.

Following the DTED approach in [24], $\mathcal{SU}_i$ can detect the usage of f_k at $\mathcal{PU}$ by comparing the energy of the received signal $\mathbf{r}_i^{(SS)}[k]$ at f_k with two corresponding energy thresholds $\mathcal{E}_{1,i}[k]$ and $\mathcal{E}_{2,i}[k]$, where $\mathcal{E}_{1,i}[k] < \mathcal{E}_{2,i}[k]$. The idea behind using double thresholds is that when the SUs cannot make a spectrum sensing decision with a good level of confidence (i.e. when the signal energy level lies between the two thresholds) then the decision, if made, would not be reliable. Therefore, to save bandwidth by reducing the reporting load to the FC, it is better not to send low-confidence sensing decisions to the FC. Let $\mathcal{H}_{1,k}^{(\mathcal{SU}_i)}$ and $\mathcal{H}_{0,k}^{(\mathcal{SU}_i)}$ denote the estimated hypotheses at $\mathcal{SU}_i$ that the f_k is occupied and unoccupied, respectively, by $\mathcal{PU}$. Also, let $\mathbf{s}_i^{(SS)}$ denote the local SIV estimated at $\mathcal{SU}_i$ over the SS channel h_{PS_i}. We can formulate the k-th element

[1]FAP is defined as the probability that a SU senses a frequency band occupied by a PU given that the PU does not operate on that frequency band.

[2]MDP is defined as the probability that a SU detects a frequency band to be available given that a PU actually occupies that frequency.

[3]In the conventional DTED, no hybrid combination of the local and global decisions is performed at the SUs.

[4]Note that the noise variance estimation error may cause some performance loss, which can be coped with by using a generalised energy detector (GED) in [29].

of $\mathbf{s}_i^{(SS)}$ as

$$\mathbf{s}_i^{(SS)}[k]=\begin{cases}0, \text{ if } \psi\left[\mathbf{r}_i^{(SS)}[k]\right] \geqslant \mathcal{E}_{2,i}[k], \text{ i.e. } \mathcal{H}_{1,k}^{(\mathcal{SU}_i)},\\ 1, \text{ if } \psi\left[\mathbf{r}_i^{(SS)}[k]\right] < \mathcal{E}_{1,i}[k], \text{ i.e. } \mathcal{H}_{0,k}^{(\mathcal{SU}_i)},\\ \psi\left[\mathbf{r}_i^{(SS)}[k]\right], \text{ otherwise,}\end{cases} \quad (2)$$

where $\psi[.]$ is the energy measurement of a signal. For convenience, let us denote the p-th binary and q-th energy values of $\mathbf{s}_i^{(SS)}$, $\{p,q\} \in \{1,2,\ldots,K\}$, by $\mathbf{s}_{b,i}^{(SS)}[p]$ and $\mathbf{s}_{e,i}^{(SS)}[q]$, respectively.

III. Proposed Hybrid Double-Threshold based Energy Detection

The proposed HDTED scheme for the CSS consists of three phases as follows:

A. Sensing Phase

In SS phase, each $\mathcal{SU}_i$, $i=1,2,\ldots,N$, locally senses the available frequency bands of $\mathcal{PU}$ over the SS channel h_{PS_i}, and then returns either a binary decision or (in case of no binary decision) a real energy value in the form of an SIV denoted by $\mathbf{s}_i^{(SS)}$ (see (2)). Without loss of generality, let us assume that, at f_k, $k=1,2,\ldots,K$, there are $N_{b,k}$ and $N_{e,k}=(N-N_{b,k})$ of $\{\mathcal{SU}_i\}$ making binary and no decisions, respectively, in the SS phase.

B. Reporting Phase

Over the RP channels, only $\{\mathcal{SU}_{i_b}\}$, $i_b=1,2,\ldots,N_{b,k}$, with binary decisions of the k-th frequency band forward $\{\mathbf{s}_{b,i_b}^{(SS)}[k]\}$ to $\mathcal{FC}$. The received signals at $\mathcal{FC}$ from $\mathcal{SU}_{i_b}$ can thus be written by

$$\mathbf{r}_{i_b}^{(RP)}[k]=\sqrt{\Lambda_{i_b}}h_{S_{i_b}F}\mathbf{x}_{b,i_b}^{(SS)}[k]+\mathbf{n}_{i_b}^{(RP)}[k], \quad (3)$$

where Λ_{i_b} is the transmission power of $\mathcal{SU}_{i_b}$, $\mathbf{x}_{b,i_b}^{(SS)}$ is the binary phase shift keying (BPSK) modulated version[5] of $\mathbf{s}_{b,i_b}^{(SS)}$ and $\mathbf{n}_{i_b}^{(RP)}$ is the independent CSCG noise vector at $\mathcal{FC}$ over the RP channel with each entry having zero mean and variance of N_0.

Then, $\mathcal{FC}$ processes to decode the received signals from each $\mathcal{SU}_{i_b}$ with respect to f_k as $\mathbf{s}_{i_b}^{(RP)}[k]$. Binary combining all the decoded SIVs $\{\mathbf{s}_{i_b}^{(RP)}\}$ from all $\{\mathcal{SU}_{i_b}\}$, $\mathcal{FC}$ makes a global decision using OR rule[6] as follows:

$$\mathbf{s}_{FC}[k]=\begin{cases}0, \text{ if } \sum_{i_b=1}^{N_{b,k}}\mathbf{s}_{i_b}^{(RP)}[k] < N_{b,k}, \text{ i.e. } \mathcal{H}_{1,k}^{(\mathcal{FC})},\\ 1, \text{ otherwise, i.e. } \mathcal{H}_{0,k}^{(\mathcal{FC})},\end{cases} \quad (4)$$

where $\mathbf{s}_{FC}$ of length K denotes the global SIV estimated at $\mathcal{FC}$. Here, $\mathcal{H}_{1,k}^{(\mathcal{FC})}$ and $\mathcal{H}_{0,k}^{(\mathcal{FC})}$ denote the estimated hypotheses at $\mathcal{FC}$ of f_k occupied or unoccupied, respectively, by $\mathcal{PU}$.

[5]For simplicity, BPSK modulation is used in our work for the signalling. The proposed scheme would be straightforwardly extended with various channel coding techniques.

[6]The OR rule was shown in [30] to give the best CSS performance compared to the AND and majority rules.

C. Backward Phase

In the BW phase, $\mathcal{FC}$ broadcasts the global SIV to all $\{\mathcal{SU}_i\}$ over BW channels[7]. The received signal at $\mathcal{SU}_i$ can be written by

$$\mathbf{r}_i^{(BW)}=\sqrt{\Lambda_{FS}}h_{FS_i}\mathbf{x}_{FC}+\mathbf{n}_i^{(BW)}, \quad (5)$$

where Λ_{FC} is the transmission power of $\mathcal{FC}$, $\mathbf{x}_{FC}$ is the BPSK modulated version of $\mathbf{s}_{FC}$ and $\mathbf{n}_i^{(BW)}$ is the independent CSCG noise vector at $\mathcal{SU}_i$ over the BW channel with each entry having zero mean and variance of N_0. Then, $\mathcal{SU}_i$ decodes the received signal from $\mathcal{FC}$ as $\mathbf{s}_i^{(BW)}$.

What is novel in the proposed HDTED scheme for the CSS is that, in the BW phase, each SU makes the final decision by combining both its local decision in the SS phase and the global decision at the FC. As the local SIV at the SUs could consist of either binary or energy values (see (2)), the final decision can be accordingly made using various methods as follows:

1) At SUs having binary decisions in SS phase: At $\{\mathcal{SU}_{i_b}\}$ with binary SIV, let us denote the weight in making the final decision by ω_{i_b}, where $0<\omega_{i_b}<1$. We then have the following two cases:

Case 1. Equal weights in making the final decision (i.e. $\omega_{i_b}=1/2$): In this case, the final decision at $\mathcal{SU}_{i_b}$ is made as follows:

$$\mathbf{s}_{SU_{b,i_b}}[k]=\begin{cases}0, \text{ if } (\mathbf{s}_{b,i_b}^{(SS)}[k]+\mathbf{s}_{i_b}^{(BW)}[k]) < 2, \text{ i.e. } \bar{\mathcal{H}}_{1,k}^{(\mathcal{SU}_{b,i_b})},\\ 1, \text{ otherwise, i.e. } \bar{\mathcal{H}}_{0,k}^{(\mathcal{SU}_{b,i_b})},\end{cases} \quad (6)$$

where $\mathbf{s}_{SU_{b,i_b}}$ denotes the final hybrid SIV at $\mathcal{SU}_{i_b}$ having local binary decision, and, $\bar{\mathcal{H}}_{1,k}^{(\mathcal{SU}_{b,i_b})}$ and $\bar{\mathcal{H}}_{0,k}^{(\mathcal{SU}_{b,i_b})}$ denote the globally hybrid-estimated hypotheses at $\mathcal{SU}_{i_b}$ of f_k occupied and unoccupied, respectively, by $\mathcal{PU}$ considering both the local and global binary SIVs. The principle of (6) is that f_k is unavailable at $\mathcal{SU}_{i_b}$ if either the local binary decision in the SS phase or the global binary decision in the BW phase indicates its occupancy at $\mathcal{PU}$.

Case 2. Unequal weights in making the final decision (i.e. $\omega_{i_b}\neq 1/2$): Let τ_{0,i_b} denote an threshold for the final decision at $\mathcal{SU}_{i_b}$. The final hybrid SIV can be determined by

$$\mathbf{s}_{SU_{b,i_b}}[k]=\begin{cases}0, \text{if } \omega_{i_b}\mathbf{s}_{e,i_b}^{(SS)}[k]+(1-\omega_{i_b})\mathbf{s}_{i_b}^{(BW)}[k] \geqslant \tau_{0,i_b}[k],\\ \qquad\qquad \text{i.e. } \bar{\mathcal{H}}_{1,k}^{(\mathcal{SU}_{b,i_b})},\\ 1, \text{ otherwise, i.e. } \bar{\mathcal{H}}_{0,k}^{(\mathcal{SU}_{b,i_b})}.\end{cases} \quad (7)$$

In (7), the weight ω_{i_b} and the threshold τ_{0,i_b} are both considered in making the final decision on the availability of f_k at $\mathcal{SU}_{i_b}$[8].

[7]Note that, with a large number of SUs, $\mathcal{FC}$ can make a global decision on all frequency bands based on the received signals from $\{\mathcal{SU}_i\}$.

[8]It is noted that ω_{i_b} need to be optimised and τ_{0,i_b} also need to be determined to achieve a target sensing reliability. However, this is beyond the scope of our work where our main aim is to improve the reliability of the spectrum sensing by exploiting both the LSS at the SU itself and CSS feedback from the FC.

2) At SUs having no binary decisions in SS phase: At $\{\mathcal{SU}_{i_e}\}$ with no binary decisions in the SS phase, the final decision at each of $\{\mathcal{SU}_{i_e}\}$ is made upon its real energy value $\mathbf{s}_{e,i_e}^{(SS)}$ (see (2)) and the global binary SIV $\mathbf{s}_{i_e}^{(BW)}$ as follows:

$$\mathbf{s}_{SU_{e,i_e}}[k] = \begin{cases} 1, \text{ if } \mathbf{s}_{i_e}^{(BW)}[k]=1 \text{ and } \mathbf{s}_{e,i_e}^{(SS)}[k] < \mathcal{E}_{0,i_e}[k], \\ \qquad\qquad\qquad\qquad \text{i.e. } \bar{\mathcal{H}}_{0,k}^{(\mathcal{SU}_{e,i_e})}, \\ 0, \text{ otherwise, i.e. } \bar{\mathcal{H}}_{1,k}^{(\mathcal{SU}_{e,i_e})}, \end{cases} \tag{8}$$

where $\mathbf{s}_{SU_{e,i_e}}$ denotes the final hybrid SIV at $\mathcal{SU}_{i_e}$ with respect to the energy value $\mathbf{s}_{e,i_e}^{(SS)}$, $\mathcal{E}_{0,i_e}[k]$ denotes the energy threshold for the final decision at $\mathcal{SU}_{i_e}$ which can be selected in the range $(\mathcal{E}_{1,i_e}[k], \mathcal{E}_{2,i_e}[k])$, and, $\bar{\mathcal{H}}_{1,k}^{(\mathcal{SU}_{e,i_e})}$ and $\bar{\mathcal{H}}_{0,k}^{(\mathcal{SU}_{e,i_e})}$ denote the globally estimated hypotheses at $\mathcal{SU}_{i_e}$ of f_k occupied and unoccupied, respectively, by $\mathcal{PU}$. The threshold $\mathcal{E}_{0,i_e}[k]$ is used to make a final decision based on both the global binary decision received from $\mathcal{FC}$ and their own energy values in the SS phase. In (8), the principle of the final detection is that f_k is available at $\mathcal{SU}_{i_e}$ if both the global binary decision indicates its availability and the local energy value detected in the SS phase is less than a certain threshold between $\mathcal{E}_{1,i_e}[k]$ and $\mathcal{E}_{2,i_e}[k]$. Unequal weighting can be similarly applied to this scenario to reflect the level of confidence between the local and global decisions.

For clarity, let us consider the equal-weight scenario. The final decision for the availability of f_k at $\{\mathcal{SU}_i\}$ consisting of both $\{\mathcal{SU}_{i_b}\}$ and $\{\mathcal{SU}_{i_e}\}$ is summarised in Table I.

TABLE I: Final decision at $\{\mathcal{SU}_i\}$.

	$\mathbf{s}_i^{(BW)}[k]=0$	$\mathbf{s}_i^{(BW)}[k]=1$
$\mathbf{s}_{b,i_b}^{(SS)}[k]=0$	0	0
$\mathbf{s}_{b,i_b}^{(SS)}[k]=1$	0	1
$\mathcal{E}_{1,i_e}[k] \leqslant \mathbf{s}_{e,i_e}^{(SS)}[k] < \mathcal{E}_{0,i_e}[k]$	0	1
$\mathcal{E}_{0,i_e}[k] \leqslant \mathbf{s}_{e,i_e}^{(SS)}[k] < \mathcal{E}_{2,i_e}[k]$	0	0

Remark 1 (*Higher Reliability in Spectrum Sensing*)**.** The proposed HDTED scheme for the CSS can determine the availability of frequency bands more reliably than the CDTED scheme (e.g. [24], [25], [27], [28]). In the CDTED scheme, the global SIV received at $\mathcal{SU}_i$ from $\mathcal{FC}$ is also the final SIV, which means that the decision at $\mathcal{SU}_i$ depends totally on the decision at $\mathcal{FC}$. Instead, in our proposed HDTED scheme, the final SIV at $\mathcal{SU}_i$ is the hybrid combination of detection of the SIVs obtained from both the LSS and CSS. As shown in (6) the hypothesis $\bar{\mathcal{H}}_{0,k}^{(\mathcal{SU}_{b,i_b})}$ at $\{\mathcal{SU}_{i_b}\}$ is decided by $\mathbf{s}_{SU_{b,i_b}}[k]=1$ if $\mathbf{s}_{b,i_b}^{(SS)}[k]=1$ and $\mathbf{s}_{i_b}^{(BW)}[k]=1$, which correspond to the hypotheses $\mathcal{H}_{0,k}^{(\mathcal{SU}_i)}$ and $\mathcal{H}_{0,k}^{(\mathcal{FC})}$ obtained from (2) and (4), respectively. This intuitively results in higher reliability in spectrum sensing with the proposed HDTED scheme. For $\{\mathcal{SU}_{i_e}\}$, let us consider the scenario that f_k is occupied at $\mathcal{PU}$. If the global decision from $\mathcal{FC}$ is $\mathbf{s}_{i_e}^{(BW)}[k]=1$, conventionally the decision at $\{\mathcal{SU}_{i_e}\}$ is that f_k is available since there is no local binary decision at $\{\mathcal{SU}_{i_e}\}$. However, in the proposed HDTED, as shown in (8), the energy value at $\{\mathcal{SU}_{i_e}\}$ with threshold $\mathcal{E}_{0,i_e}[k]$ is taken into account in the final detection, which accordingly results in a more reliable spectrum sensing.

IV. Performance Analysis of HDTED for CSS

A. Exact Closed-Form Expression of FAP and MDP

In this subsection, we derive the expressions of two performance metrics of the HDTED for the CSS in CR networks including FAP and MDP over a practical scenario where all the SS, RP and BW channels are characterised by Rayleigh flat fading channels. For convenience, let $P_f^{(A)}$ and $P_m^{(A)}$, $A \in \{\mathcal{SU}_i, \mathcal{FC}\}$, $i=1,2,\ldots,N$, denote the FAP and MDP, respectively, at node A.

For the LSS at $\mathcal{SU}_i$, let us first consider only a threshold $\mathcal{E}_{t,i}[k]$, $t=0,1,2$, $k=1,2,\ldots,K$. The average FAP and MDP of the f_k over the SS channels with respect to $\mathcal{E}_{t,i}[k]$ are respectively given by [31]

$$\begin{aligned} P_{f,t}^{(\mathcal{SU}_i)}[k] &= \Pr\left\{\psi\left[\mathbf{r}_i^{(SS)}[k]\right] \geqslant \mathcal{E}_{t,i}[k] | \mathcal{H}_{0,k}^{(\mathcal{PU})}\right\} \\ &= \frac{\Gamma\left(\mu, \frac{\mathcal{E}_{t,i}[k]}{2N_0}\right)}{\Gamma(\mu)} \triangleq \varphi(\mathcal{E}_{t,i}[k]), \end{aligned} \tag{9}$$

$$\begin{aligned} &P_{m,t}^{(\mathcal{SU}_i)}[k] = \Pr\left\{\psi\left[\mathbf{r}_i^{(SS)}[k]\right] < \mathcal{E}_{t,i}[k] | \mathcal{H}_{1,k}^{(\mathcal{PU})}\right\} \\ &= 1 - e^{-\frac{\mathcal{E}_{t,i}[k]}{2N_0}} \sum_{l=0}^{\mu-2} \frac{\mathcal{E}_{t,i}^l[k]}{l! 2^l N_0^l} - \left(\frac{N_0+\gamma_{PS_i}^{(\mathcal{SU}_i)}}{\gamma_{PS_i}^{(\mathcal{SU}_i)}}\right)^{\mu-1} \\ &\times \left[e^{-\frac{\mathcal{E}_{t,i}[k]}{2\left(N_0+\gamma_{PS_i}^{(\mathcal{SU}_i)}\right)}} - e^{-\frac{\mathcal{E}_{t,i}[k]}{2N_0}} \sum_{l=0}^{\mu-2} \frac{\mathcal{E}_{t,i}^l[k](\gamma_{PS_i}^{(\mathcal{SU}_i)})^l}{l! 2^l N_0^l \left(N_0+\gamma_{PS_i}^{(\mathcal{SU}_i)}\right)^l}\right] \\ &\triangleq \chi(\mathcal{E}_{t,i}[k], \gamma_{PS_i}^{(\mathcal{SU}_i)}), \end{aligned} \tag{10}$$

where μ is the time-bandwidth product of the energy detector, $\gamma_{PS_i}^{(\mathcal{SU}_i)}$ is average signal-to-noise ratio (SNR) at $\mathcal{SU}_i$ over the SS channel h_{PS_i}, $\Gamma(\cdot)$ is the gamma function [32, eq. (8.310.1)] and $\Gamma(\cdot,\cdot)$ is the upper incomplete gamma function [32, eq. (8.350.2)]. For brevity and w.l.o.g., the index of the frequency band (i.e. k) is omitted in the rest of the paper.

Let us denote ζ_f and ζ_m as the target FAP amd MDP[9], respectively, which are assumed to be equal at all $\{\mathcal{SU}_i\}$ and independent of the frequency bands. Also, let us assume that the noise variance, i.e. N_0, varies in the range $[N_{0,1}, N_{0,2}]$ where $0 < N_{0,1} < N_{0,2}$. From (9) and (10), $\mathcal{E}_{t,i}$, $t=1,2$, can be determined by either

$$\mathcal{E}_{t,i} = 2N_{0,t}\Gamma^{-1}(\mu, \zeta_f\Gamma(\mu)), \tag{11}$$

or

$$\mathcal{E}_{t,i} = \mathcal{E}_{t,i} \left| \chi(\mathcal{E}_{t,i}, \gamma_{PS_i}^{(\mathcal{SU}_i)}) = \zeta_m, \right. \tag{12}$$

where $\Gamma^{-1}(\cdot,\cdot)$ denotes the inverse of the upper incomplete gamma function. Therefore, taking into account both thresholds $\mathcal{E}_1$ and $\mathcal{E}_2$ for the LSS at $\mathcal{SU}_{i_b}$, $i_b=1,2,\ldots,N_b$, the

[9]Note that, given the target MDP, the energy threshold can be numerically determined by (12). However, due to the complexity of the numerical searching, the target FAP is used in this paper for tractable solution.

FAP and MDP of the HDTED with binary decision are given by

$$P_f^{(\mathcal{SU}_{i_b})} = \Pr\left\{\psi\left[r_{i_b}^{(SS)}\right] \geqslant \mathcal{E}_2 | \mathcal{H}_0^{(\mathcal{PU})}\right\} = P_{f,2}^{(\mathcal{SU}_{i_b})}, \quad (13)$$

$$P_m^{(\mathcal{SU}_{i_b})} = \Pr\left\{\psi\left[r_{i_b}^{(SS)}\right] < \mathcal{E}_1 | \mathcal{H}_1^{(\mathcal{PU})}\right\} = P_{m,1}^{(\mathcal{SU}_{i_b})}. \quad (14)$$

For real energy values at $\mathcal{SU}_{i_e}$, $i_e = 1, 2, \ldots, N_e$, let $P_{0,j}^{(\mathcal{SU}_{i_e})}$, $j = 1, 2$, denote the probability that no decision is made at $\mathcal{SU}_{i_e}$ for f_k with respect to the hypothesis $\mathcal{H}_{j,k}^{(\mathcal{PU})}$. From (9) and (10), we have

$$\begin{aligned} P_{0,0}^{(\mathcal{SU}_{i_e})} &= \Pr\left\{\mathcal{E}_1 \leqslant \psi\left[r_{i_e}^{(SS)}\right] < \mathcal{E}_2 | \mathcal{H}_0^{(\mathcal{PU})}\right\} \\ &= P_{f,1}^{(\mathcal{SU}_{i_e})} - P_{f,2}^{(\mathcal{SU}_{i_e})}, \end{aligned} \quad (15)$$

$$\begin{aligned} P_{0,1}^{(\mathcal{SU}_{i_e})} &= \Pr\left\{\mathcal{E}_1 \leqslant \psi\left[r_{i_e}^{(SS)}\right] < \mathcal{E}_2 | \mathcal{H}_1^{(\mathcal{PU})}\right\} \\ &= P_{m,2}^{(\mathcal{SU}_{i_e})} - P_{m,1}^{(\mathcal{SU}_{i_e})}. \end{aligned} \quad (16)$$

Now, let us analyse the CSS scheme performed at $\mathcal{FC}$ in the RP phase. Considering the worst scenario of failed sensing [24], there is no reporting signal from any of $\{\mathcal{SU}_i\}$. In other words, no decision is made at $\{\mathcal{SU}_i\}$. In this case, $\mathcal{FC}$ can request all $\{\mathcal{SU}_i\}$ to carry out the local spectrum sensing in the SS phase again.

Lemma 1. Denoting the probability of failed sensing under hypothesis $\mathcal{H}_0^{(\mathcal{PU})}$ and $\mathcal{H}_1^{(\mathcal{PU})}$ by ν_0 and ν_1, respectively, we have

$$\nu_0 = \prod_{i=1}^{N} P_{0,0}^{(\mathcal{SU}_i)}, \quad (17)$$

$$\nu_1 = \prod_{i=1}^{N} P_{0,1}^{(\mathcal{SU}_i)}. \quad (18)$$

Proof. See Appendix A. □

Define $\phi(x) \triangleq 1/2\left(1 - \sqrt{\frac{x}{1+x}}\right)$. We have the following finding:

Lemma 2. FAP and MDP at $\mathcal{FC}$ of the HDTED scheme over the noisy RP channels $\{h_{S_{i_b}F}\}$ are determined by

$$\begin{aligned} P_f^{(\mathcal{FC})} = (1-\nu_0)\Bigg(1 - \prod_{i_b=1}^{N_b}[(1 - P_{f,2}^{(\mathcal{SU}_{i_b})})(1 - \phi(\gamma_{S_{i_b}F}^{(\mathcal{FC})})) \\ + P_{f,2}^{(\mathcal{SU}_{i_b})}\phi(\gamma_{S_{i_b}F}^{(\mathcal{FC})})]\Bigg), \end{aligned} \quad (19)$$

$$\begin{aligned} P_m^{(\mathcal{FC})} = (1-\nu_1)\prod_{i_b=1}^{N_b}[P_{m,1}^{(\mathcal{SU}_{i_b})}(1 - \phi(\gamma_{S_{i_b}F}^{(\mathcal{FC})})) \\ + (1 - P_{m,1}^{(\mathcal{SU}_{i_b})})\phi(\gamma_{S_{i_b}F}^{(\mathcal{FC})})], \end{aligned} \quad (20)$$

respectively, where $\gamma_{S_{i_b}F}^{(\mathcal{FC})}$ denotes the SNR at $\mathcal{FC}$ over the RP channel $h_{S_{i_b}F}$.

Proof. See Appendix B. □

Remark 2 (*Impacts of Failed Sensing Probabilities*)**.** When the failed sensing is not considered, i.e. $\nu_0 = 0$ and $\nu_1 = 0$, we achieve the maximum of both the FAP and MDP at $\mathcal{FC}$ as there is at least a SU among $\{\mathcal{SU}_i\}$, $i = 1, 2, \ldots, N$, reporting the sensing data to $\mathcal{FC}$. In the scenario when ν_0 and ν_1 tend to 1, there is no decision made at any of $\{\mathcal{SU}_i\}$, and thus there is no sensing data reported from $\{\mathcal{SU}_i\}$ to $\mathcal{FC}$. In fact, from (19) and (20), the FAP and MDP at $\mathcal{FC}$ are shown to approach 0 as ν_0 and ν_1 tend to 1. Note that $\mathcal{FC}$ is exploited in this work to support the spectrum sensing. Therefore, it can be assumed that $\nu_0 \neq 1$ and $\nu_1 \neq 1$.

Then, in order to help each of $\{\mathcal{SU}_i\}$ decide the availability of spectrum, $\mathcal{FC}$ needs to forward its decision to all $\{\mathcal{SU}_i\}$ over the BW channels. Let $P_{f,b}^{(\mathcal{SU}_{i_b})}$ and $P_{m,b}^{(\mathcal{SU}_{i_b})}$ denote the FAP and MDP of the final binary decision at $\mathcal{SU}_{i_b}$, while $P_{f,e}^{(\mathcal{SU}_{i_e})}$ and $P_{m,e}^{(\mathcal{SU}_{i_e})}$ denote the FAP and MDP of the final decision at $\mathcal{SU}_{i_e}$ with real energy value over the BW channels in our proposed HDTED scheme. We then have the following findings:

Lemma 3. FAP and MDP at $\mathcal{SU}_{i_b}$ of the HDTED scheme with equal weights in the final decision over the noisy BW channels $h_{FS_{i_b}}$ are determined by

$$\begin{aligned} P_{f,b}^{(\mathcal{SU}_{i_b})} = 1 - (1 - P_{f,2}^{(\mathcal{SU}_{i_b})})[(1 - P_f^{(\mathcal{FC})})(1 - \phi(\gamma_{FS_{i_b}}^{(\mathcal{SU}_{i_b})})) \\ + P_f^{(\mathcal{FC})}\phi(\gamma_{FS_{i_b}}^{(\mathcal{SU}_{i_b})})], \end{aligned} \quad (21)$$

$$\begin{aligned} P_{m,b}^{(\mathcal{SU}_{i_b})} = P_{m,1}[P_m^{(\mathcal{FC})}(1 - \phi(\gamma_{FS_{i_b}}^{(\mathcal{SU}_{i_b})})) \\ + (1 - P_m^{(\mathcal{FC})})\phi(\gamma_{FS_{i_b}}^{(\mathcal{SU}_{i_b})})], \end{aligned} \quad (22)$$

respectively, where $\gamma_{FS_{i_b}}^{(\mathcal{SU}_{i_b})}$ denotes the SNR at $\mathcal{SU}_{i_b}$ over the BW channel $h_{FS_{i_b}}$.

Proof. See Appendix C. □

Lemma 4. FAP and MDP at $\mathcal{SU}_{i_b}$ of the HDTED scheme with unequal weights in the final decision over the noisy BW channels $h_{FS_{i_b}}$ are determined by

$$\begin{aligned} P_{f,b}^{(\mathcal{SU}_{i_b})} =& \varphi(\vartheta_1)[P_f^{(\mathcal{FC})}(1 - \phi(\gamma_{FS_{i_b}}^{(\mathcal{SU}_{i_b})})) \\ &+ (1 - P_f^{(\mathcal{FC})})\phi(\gamma_{FS_{i_b}}^{(\mathcal{SU}_{i_b})})] \\ &+ \varphi(\vartheta_2)[(1 - P_f^{(\mathcal{FC})})(1 - \phi(\gamma_{FS_{i_b}}^{(\mathcal{SU}_{i_b})})) \\ &+ P_f^{(\mathcal{FC})}\phi(\gamma_{FS_{i_b}}^{(\mathcal{SU}_{i_b})})], \end{aligned} \quad (23)$$

$$\begin{aligned} P_{m,b}^{(\mathcal{SU}_{i_b})} =& \chi(\vartheta_1, \gamma_{PS_{i_b}}^{(\mathcal{SU}_{i_b})})[(1 - P_m^{(\mathcal{FC})})(1 - \phi(\gamma_{FS_{i_b}}^{(\mathcal{SU}_{i_b})})) \\ &+ P_m^{(\mathcal{FC})}\phi(\gamma_{FS_{i_b}}^{(\mathcal{SU}_{i_b})})] \\ &+ \chi(\vartheta_2, \gamma_{PS_{i_b}}^{(\mathcal{SU}_{i_b})})[P_m^{(\mathcal{FC})}(1 - \phi(\gamma_{FS_{i_b}}^{(\mathcal{SU}_{i_b})})) \\ &+ (1 - P_m^{(\mathcal{FC})})\phi(\gamma_{FS_{i_b}}^{(\mathcal{SU}_{i_b})})], \end{aligned} \quad (24)$$

respectively, where $\vartheta_1 \triangleq \tau_{0,i_b}/\omega_{i_b}$ and $\vartheta_2 \triangleq (\tau_{0,i_b} + \omega_{i_b} - 1)/\omega_{i_b}$.

Proof. See Appendix D. □

Lemma 5. FAP and MDP at $\mathcal{SU}_{i_e}$ of the HDTED scheme over the noisy BW channels $h_{FS_{i_e}}$ are determined by

$$P_{f,e}^{(\mathcal{SU}_{i_e})} = 1 - (1 - P_{f,0}^{(\mathcal{SU}_{i_e})} + P_{f,2}^{(\mathcal{SU}_{i_e})})[(1 - P_f^{(\mathcal{FC})}) \times (1 - \phi(\gamma_{FS_{i_e}}^{(\mathcal{SU}_{i_e})})) + P_f^{(\mathcal{FC})}\phi(\gamma_{FS_{i_e}}^{(\mathcal{SU}_{i_e})})] \quad (25)$$

$$P_{m,e}^{(\mathcal{SU}_{i_e})} = (P_{m,0}^{(\mathcal{SU}_{i_e})} - P_{m,1}^{(\mathcal{SU}_{i_e})})[P_m^{(\mathcal{FC})}(1 - \phi(\gamma_{FS_{i_e}}^{(\mathcal{SU}_{i_e})})) + (1 - P_m^{(\mathcal{FC})})\phi(\gamma_{FS_{i_e}}^{(\mathcal{SU}_{i_e})})], \quad (26)$$

respectively, where $\gamma_{FS_{i_e}}^{(\mathcal{SU}_{i_e})}$ denotes the SNR at $\mathcal{SU}_{i_e}$ over the BW channel $h_{FS_{i_e}}$, and, $P_{f,0}^{(\mathcal{SU}_{i_e})}$ and $P_{m,0}^{(\mathcal{SU}_{i_e})}$ are given by (9) and (10), respectively.

Proof. From (8), the FAP and MDP at $\mathcal{SU}_{i_e}$ can be determined by

$$\begin{aligned} P_{f,e}^{(\mathcal{SU}_{i_e})} &= \Pr\{\bar{\mathcal{H}}_1^{(\mathcal{SU}_{e,i_e})} | \mathcal{H}_0^{(\mathcal{PU})}\} = \Pr\{s_{SU_{e,i_e}} = 0 | x = 0\} \\ &= 1 - \Pr\{\mathcal{E}_0 \leqslant \psi[r_{i_e}^{(SS)}] < \mathcal{E}_2 | x = 0\} \\ &\quad \times \Pr\{s_{i_e}^{(BW)} = 1 | \mathbf{x} = 0\}, \end{aligned} \quad (27)$$

$$\begin{aligned} P_{m,e}^{(\mathcal{SU}_{i_e})} &= \Pr\{\bar{\mathcal{H}}_0^{(\mathcal{SU}_{e,i_e})} | \mathcal{H}_1^{(\mathcal{PU})}\} = \Pr\{s_{SU_{e,i_e}} = 1 | \mathbf{x} \neq 0\} \\ &= \Pr\{\mathcal{E}_1 \leqslant \psi[r_{i_e}^{(SS)}] < \mathcal{E}_0 | x \neq 0\} \\ &\quad \times \Pr\{s_{i_e}^{(BW)} = 1 | x \neq 0\}, \end{aligned} \quad (28)$$

Similarly, taking into account the noisy BW channels $h_{FS_{i_e}}$, we can obtain (25) and (26). □

Corollary 1. Given the target FAP ζ_f, threshold $\mathcal{E}_0$ for the final decision at $\mathcal{SU}_{i_e}$ is computed by

$$\mathcal{E}_0 = 2N_0\Gamma^{-1}(\mu, P'_{f,0}\Gamma(\mu)), \quad (29)$$

where $P'_{f,0} = P_{f,0} | P_{f,e}^{(\mathcal{SU}_{i_e})} = \zeta_f$.

Proof. The proof is straightforwardly obtained from (9) and (25). □

Overall, the average FAP and MDP of the HDTED scheme in the whole system are given by

$$\bar{P}_f^{(\mathcal{SU})} = \frac{\sum_{i_b=1}^{N_b} P_{f,b}^{(\mathcal{SU}_{i_b})} + \sum_{i_e=1}^{N_e} P_{f,e}^{(\mathcal{SU}_{i_e})}}{N}, \quad (30)$$

$$\bar{P}_m^{(\mathcal{SU})} = \frac{\sum_{i_b=1}^{N_b} P_{m,b}^{(\mathcal{SU}_{i_b})} + \sum_{i_e=1}^{N_e} P_{m,e}^{(\mathcal{SU}_{i_e})}}{N}. \quad (31)$$

Remark 3 (*Better Sensing Performance with Our Proposed HDTED Scheme*)**.** The proposed HDTED scheme achieves a better performance than the conventional DTED scheme in terms of the MDP. In the conventional DTED scheme, no combination is performed at the SUs. In fact, following the conventional DTED scheme, the final SIV at $\mathcal{SU}_i$ is obtained from the global SIV at $\mathcal{FC}$, which means that $\mathbf{s}_{SU_i}$ depends totally on $\mathbf{s}_{FC}$. Thus, the MDP of the conventional DTED scheme at $\mathcal{SU}_i$ is computed by

$$P_{m,c}^{(\mathcal{SU}_i)} = P_m^{(\mathcal{FC})}(1 - \phi(\gamma_{FS_i}^{(\mathcal{SU}_i)})) + (1 - P_m^{(\mathcal{FC})})\phi(\gamma_{FS_i}^{(\mathcal{SU}_i)}). \quad (32)$$

From (22), (26) and (32), it can be seen that $P_{m,c}^{(\mathcal{SU}_i)} > P_{m,b}^{(\mathcal{SU}_i)}$ and $P_{m,c}^{(\mathcal{SU}_i)} > P_{m,e}^{(\mathcal{SU}_i)}$. This means our proposed HDTED scheme achieves a lower MDP than the conventional DTED scheme.

Remark 4 (*Improved Average MDP with Increased Number of SUs having Binary Local Decisions*)**.** The proposed HDTED scheme improves the average MDP at SUs when the number of SUs having binary decisions in the SS phase increases. In fact, from (20), it can be seen that $P_m^{(\mathcal{FC})}$ monotonically decreases over N_b. Thus, $P_{m,b}^{(\mathcal{SU}_{i_b})}$ and $P_{m,e}^{(\mathcal{SU}_{i_e})}$ given by (22) and (26), respectively, are decreasing functions over N_b. Accordingly, from (31), the average MDP is improved as the number of SUs having binary local decisions increases.

B. Bounds of FAP and MDP

In order to provide insightful meanings of the above derived expressions of FAP and MDP, let us investigate a specific scenario of identical channels, i.e. $\gamma_{PS_i}^{(\mathcal{SU}_i)} \triangleq \gamma_1$, $\gamma_{S_iF}^{(\mathcal{FC})} \triangleq \gamma_2$, $\gamma_{FS_i}^{(\mathcal{SU})} \triangleq \gamma_3$, $\forall i = 1, 2, \ldots, N$, and equal weights in making the decision, i.e. $\omega_{i_b} = 1/2$, $i_b = 1, 2, \ldots, N_b$. Denote the ratio of the SUs having binary decision in the LSS over the total number of the SUs by α, i.e. $\alpha = N_b/N$, $0 < \alpha \leqslant 1$. We have the following findings:

Lemma 6. The average FAP of the HDTED scheme is lower-bounded by $\bar{P}_{f,l}^{(\mathcal{SU})}$, where

$$\bar{P}_{f,l}^{(\mathcal{SU})} = 1 - [1 - \alpha(1 - \nu_0)N\phi(\gamma_2)](1 - \phi(\gamma_3))^2 - \alpha(1 - \nu_0)N\phi(\gamma_2)\phi(\gamma_3)(1 - \phi(\gamma_3)). \quad (33)$$

Proof. See Appendix E. □

Corollary 2. The lower bound of the average FAP for the HDTED scheme is in the range $(\bar{P}_{f,l_1}^{(\mathcal{SU})}, \bar{P}_{f,l_2}^{(\mathcal{SU})}]$, where

$$\bar{P}_{f,l_1}^{(\mathcal{SU})} = 1 - (1 - \phi(\gamma_3))^2, \quad (34)$$

$$\bar{P}_{f,l_2}^{(\mathcal{SU})} = 1 - [1 - (1 - \nu_0)N\phi(\gamma_2)](1 - \phi(\gamma_3))^2 - (1 - \nu_0)N\phi(\gamma_2)\phi(\gamma_3)(1 - \phi(\gamma_3)). \quad (35)$$

Proof. From (33), it can be proved that $\bar{P}_{f,l}^{(\mathcal{SU})}$ is monotonically increasing over α since $\phi(x) \leqslant 1/2$, $\forall x \geqslant 0$. Therefore, (34) and (35) are obtained as $\alpha = 0$ and $\alpha = 1$, respectively. □

Remark 5 (*Higher Lower Bound of Average FAP with Increased Number of SUs*)**.** The proposed HDTED scheme increases the lower bound of the average FAP when the number of SUs increases. In fact, from (33) in Lemma 6, it can be proved that $\bar{P}_{f,l}^{(\mathcal{SU})}$ monotonically increases over N. In other words, the increased number of SUs results in the higher lower bound of the average FAP.

Considering the two scenarios when the BW links are of very high reliability and when the number of SUs is very large, we have the following findings:

Lemma 7. When the BW links are in the high-SNR regime, i.e. $\gamma_3 \to \infty$, the average FAP and MDP of the HDTED scheme approach $\bar{P}_{f,bw_\infty}^{(\mathcal{SU})}$ and $\bar{P}_{m,bw_\infty}^{(\mathcal{SU})}$, respectively, where

$$\bar{P}_{f,bw_\infty}^{(\mathcal{SU})} = 1 - (1 - P_f^{(\mathcal{FC})})[1 - (1-\alpha)P_{f,0}^{(\mathcal{SU})} - (2\alpha - 1)P_{f,2}^{(\mathcal{SU})}], \quad (36)$$

$$\bar{P}_{m,bw_\infty}^{(\mathcal{SU})} = P_m^{(\mathcal{FC})}\left[(1-\alpha)P_{m,0}^{(\mathcal{SU})} + (2\alpha-1)P_{m,1}^{(\mathcal{SU})}\right]. \quad (37)$$

Proof. As $\gamma_3 \to \infty$, we have $\phi(\gamma_3) \to 0$. Therefore, from (21), (25) and (30), it can be proved that the average MDP approaches $\bar{P}_{f,bw_\infty}^{(\mathcal{SU})}$ as shown in (36). Similarly, $\bar{P}_{m,bw_\infty}^{(\mathcal{SU})}$ in (37) can be obtained from (22), (26) and (31). □

Lemma 8. When the number of SUs is very large, i.e. $N \to \infty$, the average FAP and MDP of the HDTED scheme approach $\bar{P}_{f,N}^{(\mathcal{SU})}$ and $\bar{P}_{m,N}^{(\mathcal{SU})}$, respectively, where

$$\begin{aligned}\bar{P}_{f,N_\infty}^{(\mathcal{SU})} &= 1 - \phi(\gamma_3)(1-\phi(\gamma_3)) \\ &\quad \times [1 - (1-\alpha)P_{f,0}^{(\mathcal{SU})} - (2\alpha-1)P_{f,2}^{(\mathcal{SU})}] \\ &\quad - \phi^2(\gamma_3)[(1-\alpha)P_{f,0}^{(\mathcal{SU})} + (2\alpha-1)P_{f,2}^{(\mathcal{SU})}], \end{aligned} \quad (38)$$

$$\begin{aligned}\bar{P}_{m,N_\infty}^{(\mathcal{SU})} &= \phi(\gamma_3)(1-\phi(\gamma_3))[(1-\alpha)P_{m,0}^{(\mathcal{SU})} + (2\alpha-1)P_{m,1}^{(\mathcal{SU})}] \\ &\quad + \phi^2(\gamma_3)[1 - (1-\alpha)P_{m,0}^{(\mathcal{SU})} - (2\alpha-1)P_{m,1}^{(\mathcal{SU})}]. \end{aligned} \quad (39)$$

Proof. As $N \to \infty$, we have $P_f^{(\mathcal{FC})} \to 1$ and $P_m^{(\mathcal{FC})} \to 0$. Substituting into (21), (22), (25), (26), (30) and (31), we obtain $\bar{P}_{f,N_\infty}^{(\mathcal{SU})}$ and $\bar{P}_{m,N_\infty}^{(\mathcal{SU})}$ as shown in (38) and (39). □

C. Optimal User Selection Algorithm for RP Phase

In Lemma 3, it can be shown that the FAP and MDP at $\mathcal{SU}_{i_b}$, $i_b = 1, 2, \ldots, N_b$, monotonically increase and decrease, respectively, as the number of $\{\mathcal{SU}_{i_b}\}$ increases. Thus, from (30) and (31), given a fixed total number of SUs in the whole network (i.e. N), the FAP and MDP of the HDTED scheme monotonically increase and decrease, respectively, over N_b. This means the ratio $\alpha = N_b/N$ can be adjusted for a target FAP instead of using all $\{\mathcal{SU}_{i_b}\}$ in the RP phase, which accordingly reduces the number of forwarding bits to the $\mathcal{FC}$.

In this subsection, let us first find the optimal value of α. An optimal user selection algorithm is then proposed for the RP phase. We have the following finding:

Lemma 9. In order to achieve the target FAP ζ_f, the ratio α should be smaller than or equal to α_u and the SNR of the BW links γ_3 should be greater than or equal to $\gamma_{3,l}$, where

$$\alpha_u = \frac{\zeta_f + (1-\phi(\gamma_3))^2 - 1}{(1-\nu_0)N\phi(\gamma_2)(1-\phi(\gamma_3))(1-2\phi(\gamma_3))}, \quad (40)$$

$$\gamma_{3,l} = \phi^{-1}\left(1 - \sqrt{1-\zeta_f}\right), \quad (41)$$

where $\phi^{-1}(\cdot)$ denotes the inverse of function $\phi(x)$.

Proof. See Appendix F. □

Let us denote the maximum number of SUs selected for the RP phase by N_b' ($N_b' \leqslant N_b$). From Lemma 9, N_b' can be determined as

$$N_b' = \lfloor \alpha_u N \rfloor, \quad (42)$$

where $\lfloor \cdot \rfloor$ denotes the floor function. Additionally, from (22), (26) and (31), it can be shown that the average MDP decreases as a function of the SNR of the SS links. Therefore, to achieve the lowest average MDP for a given target FAP (i.e. ζ_f), N_b' SUs having the highest SNRs in the SS phase should be selected for the RP phase[10]. The optimal user selection algorithm for the RP phase to achieve a target FAP is summarised in Algorithm 1.

Algorithm 1 Optimal user selection algorithm for RP phase to achieve a target FAP ζ_f

if $\gamma_3 < \phi^{-1}\left(1 - \sqrt{1-\zeta_f}\right)$ **then**
  Target FAP ζ_f can not be met.
else
  Determine α_u as in (40)
  Determine $N_b' = \lfloor \alpha_u N \rfloor$
  Select N_b' SUs having the highest SNRs in the SS phase.
end if

D. Complexity Analysis

In this subsection, we analyse the complexity of the proposed HDTED scheme in terms of the number of signaling bits and the number of computational operations (e.g. AND logic, addition and comparator circuit) for the CSS[11].

In the SS phase, it can be observed in (2) that $2K$ comparators are required at each of $\{\mathcal{SU}_i\}$, $i = 1, 2, \ldots, N$, to sense the usage of K frequency bands. With HDTED scheme and optimal user selection for the RP phase, only $\{\mathcal{SU}_{i_b'}\}$, $i_b' = 1, 2, \ldots, N_{b,k}'$ ($N_{b,k}' \leqslant N_{b,k}$), forwards the binary decisions of f_k, $k = 1, 2, \ldots, K$, to $\mathcal{FC}$, which means there are $\sum_{k=1}^{K} N_{b,k}'$ signaling bits in the RP phase. At the $\mathcal{FC}$, as shown in (4), a comparator and an addition operation are required for each of $\{f_k\}$. In order to broadcast the global SIV of K frequency bands to all $\{\mathcal{SU}_i\}$, it can be seen that the $\mathcal{FC}$ requires K signaling bits. Also, in the BW phase, from (6) and (8), there are an addition and a comparator at each of $\{\mathcal{SU}_{i_b}\}$, while $\{\mathcal{SU}_{i_e}\}$, $i_e = 1, 2, \ldots, N_{e,k}$, requires an AND logic and two comparators.

Let $\mathcal{T}_b$ and $\mathcal{T}_o$ denote the total number of signaling bits and the total number of computational operations, respectively. We then have

$$\mathcal{T}_b = K + \sum_{k=1}^{K} N_{b,k}', \quad (43)$$

$$\mathcal{T}_o = 4K + 2\sum_{k=1}^{K} N_{b,k} + 3\sum_{k=1}^{K} N_{e,k}. \quad (44)$$

Remark 6 (*Complexity Comparison*)**.** Let us compare the complexity of the proposed HDTED scheme with the following DTED schemes:

- *Scheme 1*: Binary combination at $\mathcal{FC}$ and no combination at $\{\mathcal{SU}_i\}$ over BW links.

[10]It is noted that the user selection can be realised in a centralised manner with the assistance of a coordinator, e.g. $\mathcal{FC}$.

[11]The complexity also reflects the sensing duration, which can be optimised following the approach in [33].

- *Scheme 2*: Binary combination at $\mathcal{FC}$ and binary combination at $\{\mathcal{SU}_{i_b}\}$ over BW links.
- *Scheme 3*: Hybrid combination at $\mathcal{FC}$ and no combination at $\{\mathcal{SU}_i\}$ over BW links.
- *Scheme 4*: Hybrid combination at $\mathcal{FC}$ and binary combination at $\{\mathcal{SU}_{i_b}\}$ over BW links.

For convenience, let $\mathcal{T}_{b,i}$ and $\mathcal{T}_{o,i}$, $i = 1, 2, 3, 4$, denote the total number of signaling bits and the total number of computational operations, respectively, in Scheme i. It can be seen that Schemes 1 and 2 require the same number of signaling bits, which are higher or equal to that in the HDTED scheme (i.e. $\mathcal{T}_{b,1} = \mathcal{T}_{b,2} \geqslant \mathcal{T}_b$) since $N_{b,k} \geqslant N'_{b,k}$. However, Schemes 1 and 2 requires a smaller computational operations of $\mathcal{T}_{o,1} = 4K$ and $\mathcal{T}_{o,2} = 4K + 2\sum_{k=1}^{K} N_{b,k}$, respectively. In Schemes 3 and 4, it is noted that more signaling bits are required to send the energy values from $\{\mathcal{SU}_{i_e}\}$, $i_e = 1, 2, \ldots, N_{e,k}$, $k = 1, 2, \ldots, K$, to $\mathcal{FC}$. Let δ denote the number of bits used for representing 2^δ quantisation levels for an energy sample. The total number of signaling bits in both Schemes 3 and 4 can be obtained as $\mathcal{T}_{b,3} = \mathcal{T}_{b,4} = K + \sum_{k=1}^{K} N_{b,k} + \delta \sum_{k=1}^{K} N_{e,k}$, which is much larger than the HDTED scheme, Scheme 1 and Scheme 2, especially when δ is large. Similar to Schemes 1 and 2, Schemes 3 and 4 require $\mathcal{T}_{o,3} = 4K$ and $\mathcal{T}_{o,4} = 4K + 2\sum_{k=1}^{K} N_{b,k}$ computational operations, respectively. For clarity, Table II summarises the complexity comparison between different HDTED schemes with a specific example of $N = 10$, $K = 7$, $N_{b,k} = 8$, $N_{e,k} = 2$, $N'_{b,k} = 3$ and $\delta = 3$. Overall, the proposed HDTED scheme requires a higher complexity computational processing but a smaller number of signaling bits in comparison to other schemes. With the rapid growth of integrated circuits for high-complexity computations, the delay caused by the computation operations in the proposed scheme is negligible when compared to the complexity caused by the transmission of a higher number of signaling bits.

V. Numerical Results

In this section, we evaluate the FAP and MDP performance of various DTED schemes for CSS. Also, the analytical formulations and observations in Section IV are now discussed and validated. Specifically, the proposed HDTED scheme is investigated in light of four schemes[12] as described in Remark 6.

A. Complementary Receiver Operating Characteristic of DTED Schemes

In Figs. 2, 3 and 4, the complementary receiver operating characteristic (CROC)[13] is illustrated for various DTED schemes with respect to different number of SUs having either binary decisions or no decisions in the SS phase. We assume that there are totally 10 SUs (i.e. $N = 10$) and the time-bandwidth product of the energy detector is $\mu = 5$.

[12]Note that the hybrid combination at $\mathcal{FC}$ in Schemes 3 and 4 is realised as in [27] where both the binary and energy values are taken into account in making the decision at $\mathcal{FC}$.

[13]The CROC is defined as the relationship between the average MDP and the average FAP (e.g. in [31]).

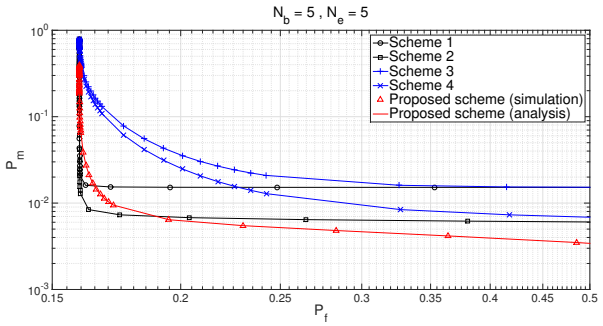

Fig. 2: Performance comparison of DTED schemes when $N_b = N_e = 5$.

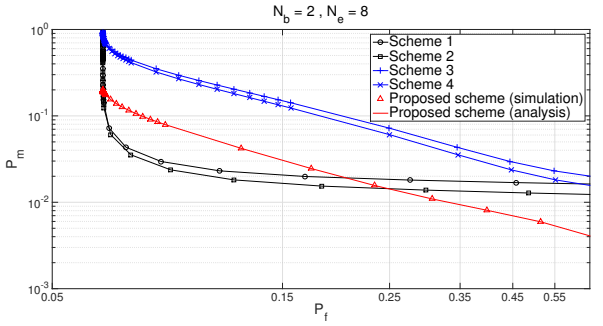

Fig. 3: Performance comparison of DTED schemes when $N_b = 2$ and $N_e = 8$.

The SNRs of the SS, RP and BW channels are assumed as $\{\gamma_{PS_i}^{(\mathcal{SU}_i)}\} = \{-8, -16, -7, -19, -5, -12, -20, -15, -14, -13\}$ dB, $\{\gamma_{S_iF}^{(\mathcal{FC})}\} = \{12, 8, 9, 7, 8, 10, 9, 14, 6, 9\}$ dB and $\{\gamma_{FS_i}^{(\mathcal{SU}_i)}\} = \{10, 12, 12, 11, 10, 12, 13, 15, 14, 13\}$ dB. In Fig. 2, we consider the balanced scenario of the number of SUs having either binary decisions (i.e. N_b) or no decisions (i.e. N_e) when $N_b = N_e = 5$, while two imbalanced scenarios when $\{N_b = 2, N_e = 8\}$ and $\{N_b = 8, N_e = 2\}$ are plotted in Figs. 3 and 4, respectively. It can be observed that the proposed scheme achieves a better performance than the other schemes in terms of the MDP. This observation confirms the statements in Remarks 1 and 3 regarding the improved reliability of the proposed HDTED scheme. It can also be seen that there is a

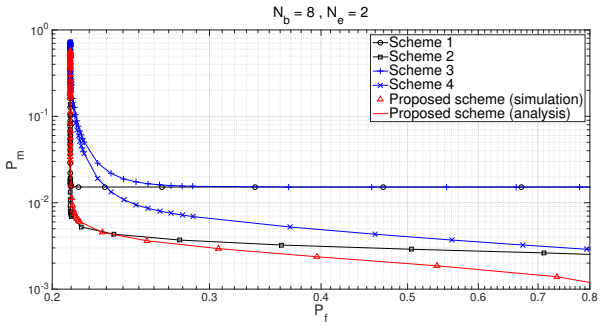

Fig. 4: Performance comparison of DTED schemes when $N_b = 8$ and $N_e = 2$.

TABLE II: Complexity comparison with a specific example of $N = 10$, $K = 7$, $N_{b,k} = 8$, $N_{e,k} = 2$, $N'_{b,k} = 3$ and $\delta = 3$.

DTED schemes	Signalling bits $\mathcal{T}_b$		Computation operations $\mathcal{T}_0$	
	General	*Example*	*General*	*Example*
Scheme 1	$K + \sum_{k=1}^{K} N_{b,k}$	63	$4K$	28
Scheme 2	$K + \sum_{k=1}^{K} N_{b,k}$	63	$4K + 2\sum_{k=1}^{K} N_{b,k}$	140
Scheme 3	$K + \sum_{k=1}^{K} N_{b,k} + \delta \sum_{k=1}^{K} N_{e,k}$	105	$4K$	28
Scheme 4	$K + \sum_{k=1}^{K} N_{b,k} + \delta \sum_{k=1}^{K} N_{e,k}$	105	$4K + 2\sum_{k=1}^{K} N_{b,k}$	140
Proposed HDTED	$K + \sum_{k=1}^{K} N'_{b,k}$	28	$4K + 2\sum_{k=1}^{K} N_{b,k} + 3\sum_{k=1}^{K} N_{e,k}$	182

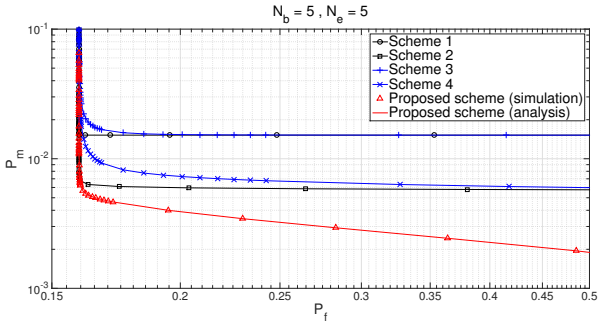

Fig. 5: Performance comparison of DTED schemes when $N_b = N_e = 5$ and high SNR of the SS channels.

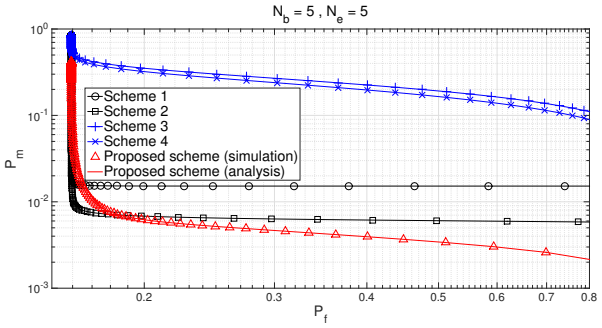

Fig. 6: Performance comparison of DTED schemes when $N_b = N_e = 5$ given target MDP.

rapid drop of the MDP at the lower values of the FAP, which is caused by the lower bound of FAP derived in Lemma 6. Additionally, the analytical results in Lemmas 3 and 5 are shown to be consistent with the simulation results.

As a further illustration, Fig. 5 plots the CROC for the scenario $N_b = N_e = 5$ at the high-SNR regime of the SS channels. The SNRs of the SS channels are assumed to be $\{\gamma_{PS_i}^{(\mathcal{SU}_i)}\} = \{8, 6, 7, 9, 5, 2, 3, 5, 4, 3\}$ dB, while other parameters are set as in Fig. 2. It can be observed that an improved MDP with a higher gain is achieved with the proposed scheme compared to the other schemes. Overall, the above observations verify the efficiency of our proposed scheme for the whole range of SNR levels in the sensing.

B. CROC of DTED Schemes w.r.t. Target MDP

Considering the target MDP in finding the energy threshold for spectrum sensing in SS phase, Fig. 6 plots the CROC performance of various DTED schemes for the scenario of $N_b = N_e = 5$. The energy threshold is determined via numerical searching method in MATLAB as in (12). It can be observed in Fig. 6 that the proposed scheme still achieves a better performance than the other schemes in terms of the MDP. This observation is consistent with the results in Fig. 2 where the target FAP is considered. However, the numerical searching requires a high computation complexity, especially with a large number of SUs. Therefore, the target FAP is selected to find the energy threshold in the rest of the numerical simulations.

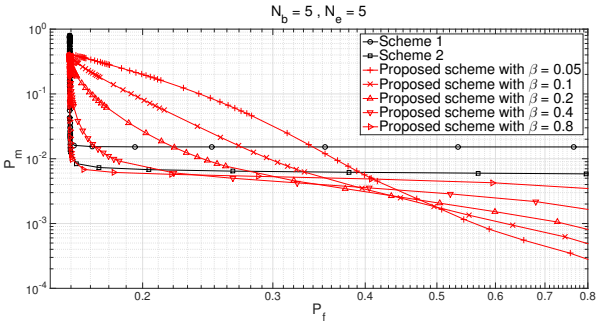

Fig. 7: Performance comparison of DTED schemes with respect to different values of $\beta = (\mathcal{E}_0 - \mathcal{E}_1)/(\mathcal{E}_2 - \mathcal{E}_1)$.

C. Effect of Energy Threshold for Final Decision on CROC Performance

Fig. 7 shows the CROC of various DTED schemes for the CSS with respect to different values of $\beta = (\mathcal{E}_0 - \mathcal{E}_1)/(\mathcal{E}_2 - \mathcal{E}_1)$. Here, β represents the relative distance between the threshold for the final decision $\mathcal{E}_0$ (see Corollary 1) and two thresholds for the local decision $\mathcal{E}_1$ and $\mathcal{E}_2$ at the SUs (see (11)). In Fig. 7, we compare the CROC of the proposed HDTED scheme with Scheme 1 and Scheme 2. We assume that $N_b = N_e = 5$ and the SNRs of the SS, RP and BW channels are similarly set as in Fig. 2. It can be observed that a lower MDP is achieved as β decreases (i.e. $\mathcal{E}_0 \to \mathcal{E}_1$), however this results in a higher FAP. In fact, this observation can be verified through Lemma 5 where the MDP and FAP at the SUs having no local decision are shown to decrease and increase, respectively, as $\mathcal{E}_0$ decreases.

D. Effect of BW Links on CSS

Figs. 8 and 9 plot the average MDP and FAP of various DTED schemes against the SNR of the BW links. A total of 10 SUs is considered and set $N_b = N_e = 5$. The SNRs of the SS and RP channels are assumed to be -10 dB and 4 dB,

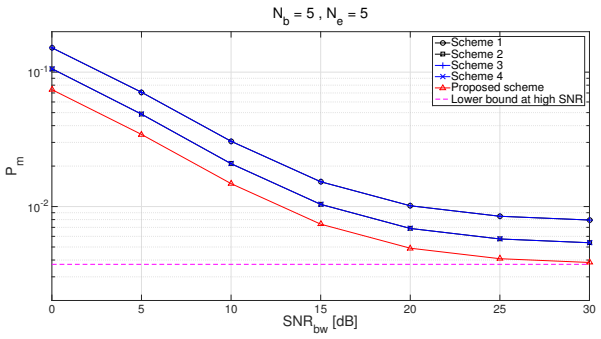

Fig. 8: MDP of DTED schemes over SNR of BW links.

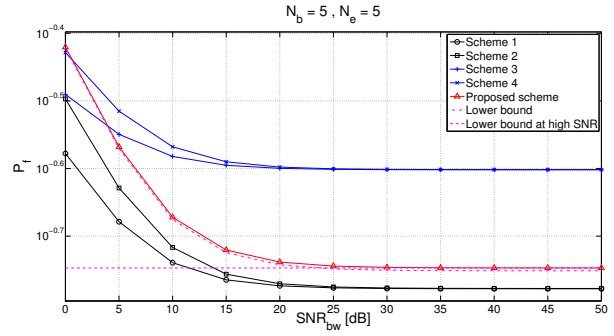

Fig. 9: FAP of DTED schemes over SNR of BW links.

respectively. In Fig. 8, it can be seen that the proposed HDTED achieves the lowest MDP compared to the other schemes for all values of the SNR of the BW links. Also, in the high SNR regime, the MDP of the proposed scheme is shown to approach the bound as shown in (37) in Lemma 7. Considering the FAP, in Fig. 9, the proposed scheme is shown to achieve a better performance compared to Schemes 3 and 4, while Schemes 1 and 2 are shown to be the best in the high SNR regime. In fact, the usage of an additional threshold in the proposed HDTED scheme is helpful in improving the reliability of the CSS in terms of the MDP, however it may cause a higher FAP. It can be also observed in Fig. 9 that the FAP of the proposed HDTED scheme is lower bounded by a curve (see (33)) and approaches the bound given by (36) in Lemma 7 for high SNR values of the BW links.

E. Effect of the Number of SUs on CSS

As shown in Figs. 10 and 11, the average MDP and FAP of various DTED schemes are plotted as functions of the total number of SUs (i.e. N), respectively. We assume that $N_b = N_e = N/2$ and the SNRs of the SS, RP and BW links are set as -10, 4 and 6 dB, respectively. It can be observed that the proposed HDTED scheme achieves the best MDP performance while all the schemes approach a similar FAP performance as N is large. Additionally, both the FAP and MDP of the proposed HDTED scheme approach the bounds given by (38) and (39), respectively, in Lemma 8. Moreover, considering the scenario when the total number of SUs is fixed, Figs. 12 and 13 shows the average MDP and FAP of various DTED schemes as functions of both N_b and N_e given $N_b + N_e = N = 30$. It

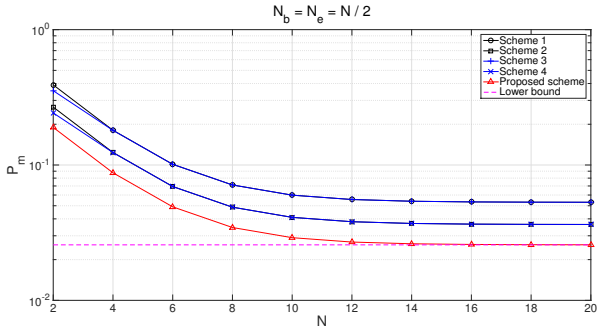

Fig. 10: MDP of DTED schemes over the number of SUs.

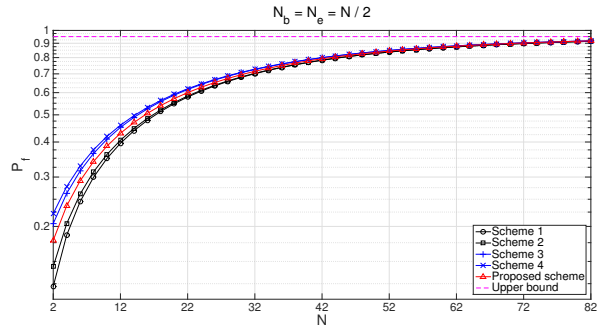

Fig. 11: FAP of DTED schemes over the number of SUs.

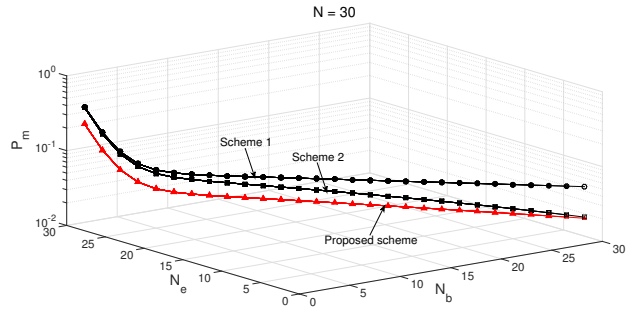

Fig. 12: MDP of DTED schemes over a pair (N_b, N_e) satisfying $N_b + N_e = N = 30$.

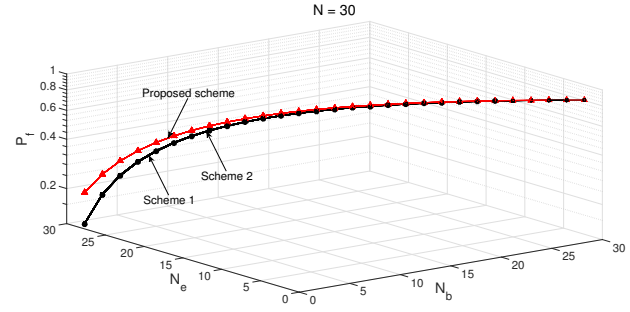

Fig. 13: FAP of DTED schemes over a pair (N_b, N_e) satisfying $N_b + N_e = N = 30$.

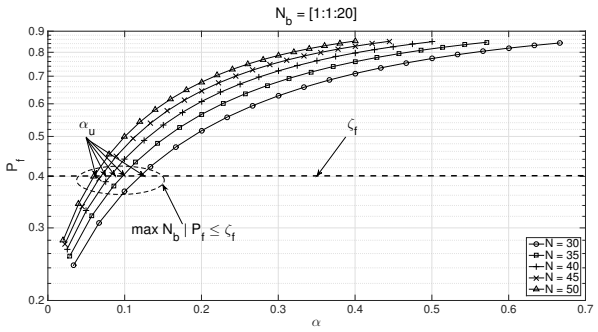

Fig. 14: FAP of HDTED scheme over the ratio α of SUs.

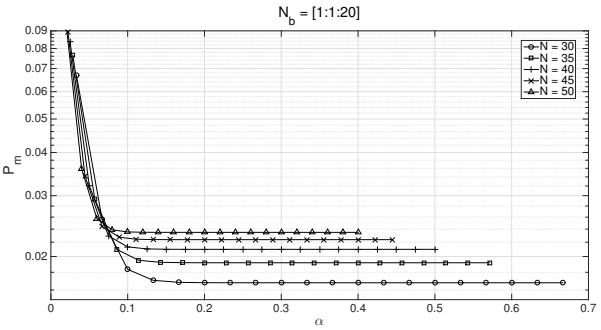

Fig. 15: MDP of HDTED schemes over the ratio α of SUs.

can be similarly observed that the proposed HDTED scheme achieves a better MDP performance compared to the other schemes while the FAP of the proposed scheme approaches a similar performance as the others as N_b increases. Also, a lower MDP is achieved as N_b increases. This observation again confirms the statement in Remark 4 about the improved average MDP achieved with increased number of SUs having binary local decisions.

F. User Selection for RP Phase

Figs. 14 and 15 plot the average FAP and MDP of the proposed HDTED scheme as functions of the ratio $\alpha = N_b/N$ with respect to different values of the total number of SUs. We assume that $N \in \{30, 35, 40, 45, 50\}$ and N_b varies in $[1, 20]$. The SNRs of the SS, RP and BW links are set as -10 dB, 4 dB and 6 dB, respectively, and the target FAP is set as $\zeta_f = 0.4$. It is observed in Fig. 14, in order to achieve the target FAP, the number of SUs selected for the RP phase should be less than or equal to 3. This observation in fact can be verified by $\lfloor \alpha_u N \rfloor$ where α_u is given by (40) in Lemma 9. Furthermore, as shown in Fig. 15, the average MDP decreases as α increases (see Remark 4). Therefore, in this scenario, 3 SUs should be selected for the RP phase to guarantee both the target FAP and the lowest MDP.

VI. Conclusions

In this paper, we have proposed a HDTED scheme to improve the performance of the CSS by exploiting both the local decisions at SUs and global decisions feedback from FC. An additional threshold has been included for making the final decision at the SUs in case there is no binary local decision made in the SS phase. An analysis of FAP and MDP for the HDTED scheme has been carried out considering the practical scenario where all channels suffer from Rayleigh fading. Specifically, closed-form expressions and bounds of the FAP and MDP have been derived. The derived expressions reflect well the impacts of the total number of the SUs, the number of the SUs having either binary or no local decisions and the quality of the links on the effectiveness of the proposed HDTED scheme for the CSS. Furthermore, an optimal user selection algorithm has been proposed for the RP phase to save the number of signaling bits not only for a lower complexity but also for a lower power transmission consumption. Additionally, numerical results for various DTED schemes with respect to various variants have been provided, which have confirmed the analytical results. For future work, we will investigate the performance of the proposed HDTED scheme taking into account the effects of noise variance uncertainty.

Appendix A
Proof of Lemma 1

As there is no reporting signal from any of $\}\mathcal{SU}\}$, $i = 1, 2, \ldots, N$, in the worst scenario of failed sensing, the probability of failed sensing under hypothesis $\mathcal{H}_0^{(\mathcal{PU})}$ and $\mathcal{H}_1^{(\mathcal{PU})}$ can be determined by

$$\nu_0 = \Pr\{N_b = 0 | \mathcal{H}_0^{(\mathcal{PU})}\}, \tag{45}$$

$$\nu_1 = \Pr\{N_b = 0 | \mathcal{H}_1^{(\mathcal{PU})}\}. \tag{46}$$

Given i.i.d. sensing channels, from (2), we have

$$\nu_0 = \prod_{i=1}^{N} \Pr\left\{\mathcal{E}_1 \leqslant \psi\left[r_i^{(SS)}\right] < \mathcal{E}_2 | \mathcal{H}_0^{(\mathcal{PU})}\right\}, \tag{47}$$

$$\nu_1 = \prod_{i=1}^{N} \Pr\left\{\mathcal{E}_1 \leqslant \psi\left[r_i^{(SS)}\right] < \mathcal{E}_2 | \mathcal{H}_1^{(\mathcal{PU})}\right\}. \tag{48}$$

Substituting (15) and (16) into (47) and (48), we obtain ν_0 and ν_1 as in (17) and (18), respectively.

Appendix B
Proof of Lemma 2

From (4), the FAP and MDP at $\mathcal{FC}$ can be written as

$$\begin{aligned} P_f^{(\mathcal{FC})} &= \Pr\{N_b \geqslant 1 | \mathcal{H}_0^{(\mathcal{PU})}\} \Pr\{\mathcal{H}_1^{(\mathcal{FC})} | \mathcal{H}_0^{(\mathcal{PU})}\} \\ &= (1 - \nu_0) \Pr\{s_{FC} = 0 | x = 0\} \\ &= (1 - \nu_0) \left(1 - \prod_{i_b=1}^{N_b} \Pr\{s_{i_b}^{(RP)} = 1 | x = 0\}\right), \end{aligned} \tag{49}$$

$$\begin{aligned} P_m^{(\mathcal{FC})} &= \Pr\{N_b \geqslant 1 | \mathcal{H}_1^{(\mathcal{PU})}\} \Pr\{N_b \geqslant 1\} \Pr\{\mathcal{H}_0^{(\mathcal{FC})} | \mathcal{H}_1^{(\mathcal{PU})}\} \\ &= (1 - \nu_1) \Pr\{s_{FC} = 1 | x \neq 0\} \\ &= (1 - \nu_1) \prod_{i_b=1}^{N_b} \Pr\{s_{i_b}^{(RP)} = 1 | x \neq 0\}. \end{aligned} \tag{50}$$

Note that the bit error probability (BEP) for the transmission of BPSK modulated signal over a Rayleigh flat fading channel h_{AB} is given by [34]

$$P_b(E_{AB}) = \phi(\gamma), \tag{51}$$

where γ is the average SNR and $\phi(x) \triangleq \frac{1}{2}\left(1-\sqrt{\frac{x}{1+x}}\right)$. Thus, from (13), (14), (49), (50) and (51), we obtain the FAP and MDP at the FC over the noisy RP channels $\left\{h_{S_{i_b}F}\right\}$, $i_b = 1, 2, \ldots, N_b$, as (19) and (20), respectively.

Appendix C
Proof of Lemma 3

From (6), the FAP and MDP at $\mathcal{SU}_{i_b}$, $i_b = 1, 2, \ldots, N_b$, with equal weights in the final decision can be determined by

$$\begin{aligned} P_{f,b}^{(\mathcal{SU}_{i_b})} &= \Pr\{\bar{\mathcal{H}}_1^{(\mathcal{SU}_{b,i_b})} | \mathcal{H}_0^{(\mathcal{PU})}\} = \Pr\{s_{SU_{b,i_b}} = 0 | x = 0\} \\ &= 1 - \Pr\{s_{b,i_b}^{(SS)} = 1 | x = 0\} \Pr\{s_{i_b}^{(BW)} = 1 | \mathbf{x} = 0\}, \end{aligned} \tag{52}$$

$$\begin{aligned} P_{m,b}^{\mathcal{SU}_{i_b})} &= \Pr\{\bar{\mathcal{H}}_0^{(\mathcal{SU}_{b,i_b})} | \mathcal{H}_1^{(\mathcal{PU})}\} = \Pr\{s_{SU_{b,i_b}} = 1 | \mathbf{x} \neq 0\} \\ &= \Pr\{s_{b,i_b}^{(SS)} = 1 | x \neq 0\} \Pr\{s_{i_b}^{(BW)} = 1 | x \neq 0\}. \end{aligned} \tag{53}$$

Thus, the FAP and MDP at $\mathcal{SU}_{i_b}$ over the noisy BW channels $h_{FS_{i_b}}$ can be written as

$$\begin{aligned} P_{f,b}^{(\mathcal{SU}_{i_b})} = 1 - (1 - P_f^{(\mathcal{SU}_{i_b})}) [(1 - P_f^{(\mathcal{FC})})(1 - P_b(E_{FS_{i_b}})) \\ + P_f^{(\mathcal{FC})} P_b(E_{FS_{i_b}})], \end{aligned} \tag{54}$$

$$\begin{aligned} P_{m,b}^{(\mathcal{SU}_{i_b})} = P_m^{(\mathcal{SU}_{i_b})} [P_m^{(\mathcal{FC})}(1 - P_b(E_{FS_{i_b}})) \\ + (1 - P_m^{(\mathcal{FC})}) P_b(E_{FS_{i_b}})]. \end{aligned} \tag{55}$$

Substituting (13), (14) and (51) into (54) and (55), we obtain (21) and (22).

Appendix D
Proof of Lemma 4

Considering the unequal weights of the SU and FC in the final decision, from (7), the FAP and MDP at $\mathcal{SU}_{i_b}$, $i_b = 1, 2, \ldots, N_b$, can be determined by

$$\begin{aligned} P_{f,b}^{(\mathcal{SU}_{i_b})} &= \Pr\{\bar{\mathcal{H}}_1^{(\mathcal{SU}_{b,i_b})} | \mathcal{H}_0^{(\mathcal{PU})}\} = \Pr\{s_{SU_{b,i_b}} = 0 | x = 0\} \\ &= \Pr\{\omega_{i_b} \psi[r_{i_b}^{(SS)}] \geqslant \tau_{0,i_b} | x = 0\} \Pr\{s_{i_b}^{(BW)} = 0 | x = 0\} \\ &\quad + \Pr\{\omega_{i_b} \psi[r_{i_b}^{(SS)}] + 1 - \omega_{i_b} \geqslant \tau_{0,i_b} | x = 0\} \\ &\quad \times \Pr\{s_{i_b}^{(BW)} = 1 | x = 0\}, \end{aligned} \tag{56}$$

$$\begin{aligned} P_{m,b}^{\mathcal{SU}_{i_b})} &= \Pr\{\bar{\mathcal{H}}_0^{(\mathcal{SU}_{b,i_b})} | \mathcal{H}_1^{(\mathcal{PU})}\} = \Pr\{s_{SU_{b,i_b}} = 1 | x \neq 0\} \\ &= \Pr\{\omega_{i_b} \psi[r_{i_b}^{(SS)}] < \tau_{0,i_b} | x \neq 0\} \Pr\{s_{i_b}^{(BW)} = 0 | x \neq 0\} \\ &\quad + \Pr\{\omega_{i_b} \psi[r_{i_b}^{(SS)}] + 1 - \omega_{i_b} < \tau_{0,i_b} | x \neq 0\} \\ &\quad \times \Pr\{s_{i_b}^{(BW)} = 1 | x \neq 0\}. \end{aligned} \tag{57}$$

Let $\vartheta_1 \triangleq \tau_{0,i_b}/\omega_{i_b}$ and $\vartheta_2 \triangleq (\tau_{0,i_b} + \omega_{i_b} - 1)/\omega_{i_b}$. We have

$$\Pr\{\psi[r_{i_b}^{(SS)}] \geqslant \vartheta_i | x = 0\} = \varphi(\vartheta_i), \tag{58}$$

$$\Pr\{\psi[r_{i_b}^{(SS)}] < \vartheta_i | x \neq 0\} = \chi(\vartheta_i, \gamma_{PS_{i_b}}^{(\mathcal{SU}_{i_b})}), \tag{59}$$

where $\varphi(\cdot)$ and $\chi(\cdot,\cdot)$ are defined as in (9) and (10), respectively. Substituting (58) and (59) into (56) and (57), we obtain

$$P_{f,b}^{(\mathcal{SU}_{i_b})} = \varphi(\vartheta_1) P_f^{(\mathcal{FC})} + \varphi(\vartheta_2)(1 - P_f^{(\mathcal{FC})}), \tag{60}$$

$$P_{m,b}^{\mathcal{SU}_{i_b})} = \chi(\vartheta_1, \gamma_{PS_{i_b}}^{(\mathcal{SU}_{i_b})})(1 - P_m^{(\mathcal{FC})}) + \chi(\vartheta_2, \gamma_{PS_{i_b}}^{(\mathcal{SU}_{i_b})}) P_m^{(\mathcal{FC})}. \tag{61}$$

Thus, the FAP and MDP at $\mathcal{SU}_{i_b}$ over the noisy BW channels $h_{FS_{i_b}}$ can be computed as

$$\begin{aligned} P_{f,b}^{(\mathcal{SU}_{i_b})} = \varphi(\vartheta_1) [P_f^{(\mathcal{FC})}(1 - \phi(\gamma_{FS_{i_b}}^{(\mathcal{SU}_{i_b})})) \\ + (1 - P_f^{(\mathcal{FC})}) \phi(\gamma_{FS_{i_b}}^{(\mathcal{SU}_{i_b})})] \\ + \varphi(\vartheta_2) [(1 - P_f^{(\mathcal{FC})})(1 - \phi(\gamma_{FS_{i_b}}^{(\mathcal{SU}_{i_b})})) \\ + P_f^{(\mathcal{FC})} \phi(\gamma_{FS_{i_b}}^{(\mathcal{SU}_{i_b})})], \end{aligned} \tag{62}$$

$$\begin{aligned} P_{m,b}^{(\mathcal{SU}_{i_b})} = \chi(\vartheta_1, \gamma_{PS_{i_b}}^{(\mathcal{SU}_{i_b})}) [(1 - P_m^{(\mathcal{FC})})(1 - \phi(\gamma_{FS_{i_b}}^{(\mathcal{SU}_{i_b})})) \\ + P_m^{(\mathcal{FC})} \phi(\gamma_{FS_{i_b}}^{(\mathcal{SU}_{i_b})})] \\ + \chi(\vartheta_2, \gamma_{PS_{i_b}}^{(\mathcal{SU}_{i_b})}) [P_m^{(\mathcal{FC})}(1 - \phi(\gamma_{FS_{i_b}}^{(\mathcal{SU}_{i_b})})) \\ + (1 - P_m^{(\mathcal{FC})}) \phi(\gamma_{FS_{i_b}}^{(\mathcal{SU}_{i_b})})]. \end{aligned} \tag{63}$$

Appendix E
Proof of Lemma 6

Given identical channels $\gamma_{PS_i}^{(\mathcal{SU}_i)} \triangleq \gamma_1$, $\gamma_{S_iF}^{(\mathcal{FC})} \triangleq \gamma_2$ and $\gamma_{FS_i}^{(\mathcal{SU})} \triangleq \gamma_3$, $\forall i = 1, 2, \ldots, N$, we have $\phi(\gamma_{PS_i}^{(\mathcal{SU}_i)}) = \phi(\gamma_1)$, $\phi(\gamma_{S_iF}^{(\mathcal{FC})}) = \phi(\gamma_2)$ and $\phi(\gamma_{FS_i}^{(\mathcal{SU})}) = \phi(\gamma_3)$.

Also, from (9) and (9), all SUs achieve the same FAP and MDP in the LSS process, i.e. $P_{f,t}^{(\mathcal{SU}_i)} \triangleq P_{f,t}^{(\mathcal{SU})}$ and $P_{m,t}^{(\mathcal{SU}_i)} \triangleq P_{m,t}^{(\mathcal{SU})}$, $t = 0, 1, 2$.

From (21), the FAP at $\mathcal{SU}_{i_b}$, $i_b = 1, 2, \ldots, N_b$, over the BW channels can be rewritten as

$$\begin{aligned} P_{f,b}^{(\mathcal{SU})} &= 1 - \left(1 - P_{f,2}^{(\mathcal{SU})}\right)\left(1 - P_f^{(\mathcal{FC})}\right)(1 - \phi(\gamma_3))^2 \\ &\quad - \phi(\gamma_3)(1 - \phi(\gamma_3)) \left[P_{f,2}^{(\mathcal{SU})} + P_f^{(\mathcal{FC})} - 2P_{f,2}^{(\mathcal{SU})} P_f^{(\mathcal{FC})}\right] \\ &\quad - P_{f,2}^{(\mathcal{SU})} P_f^{(\mathcal{FC})} (\phi(\gamma_3))^2. \end{aligned} \tag{64}$$

It can be proved that, over Rayleigh flat fading channel, the FAP of the CSS scheme is monotonically increasing over the FAP of the LSS scheme since $\phi(\gamma_3) \leqslant 1/2$ (see (51)). Thus, $P_{f,b}^{(\mathcal{SU})}$ is lower-bounded if $P_{f,2}^{(\mathcal{SU})}$ approaches to zero.

Let $\bar{P}_{f,b}^{(\mathcal{SU})}$ denote the lower bound of $P_{f,b}^{(\mathcal{SU})}$. Then

$$\begin{aligned} \bar{P}_{f,b}^{(\mathcal{SU})} = \lim_{P_{f,2}^{(\mathcal{SU})} \to 0} P_{f,b}^{(\mathcal{SU})} = 1 - (1 - P_f^{(\mathcal{FC})})(1 - \phi(\gamma_3))^2 \\ - \phi(\gamma_3)(1 - \phi(\gamma_3)) P_f^{(\mathcal{FC})}. \end{aligned} \tag{65}$$

In (65), it can be shown that $\bar{P}_{f,b}^{(\mathcal{SU})}$ is monotonically increasing over $P_f^{(\mathcal{FC})}$, and thus is lower-bounded if $P_f^{(\mathcal{FC})}$ is lower-bounded.

Since $P_{f,2}^{(\mathcal{SU}_{i_b})} = P_{f,2}^{(\mathcal{SU})}$ and $\phi(\gamma_{S_{i_b}F}^{(\mathcal{FC})}) = \phi(\gamma_2)$, $\forall i_b = 1, 2, \ldots, N_b$, from (19), the FAP at the FC is rewritten by

$$P_f^{(\mathcal{FC})} = (1-\nu_0) \times \left[1 - [(1 - P_{f,2}^{(\mathcal{SU})})(1-\phi(\gamma_2)) + P_{f,2}^{(\mathcal{SU})}\phi(\gamma_2)]^{N_b}\right]. \quad (66)$$

Similarly, it can be proved that $P_f^{(\mathcal{FC})}$ is monotonically increasing over $P_{f,2}^{(\mathcal{SU})}$ and thus is lower-bounded by

$$\begin{aligned}\bar{P}_f^{(\mathcal{FC})} &= \lim_{P_{f,2}^{(\mathcal{SU})} \to 0} P_f^{(\mathcal{FC})} = (1-\nu_0)\left(1 - (1-\phi(\gamma_2))^{N_b}\right) \\ &\approx (1-\nu_0) N_b \phi(\gamma_2). \end{aligned} \quad (67)$$

Thus, substituting $\bar{P}_f^{(\mathcal{FC})}$ into (65), we obtain

$$\begin{aligned}\bar{P}_{f,b}^{(\mathcal{SU})} =& 1 - (1 - (1-\nu_0)N_b\phi(\gamma_2)))(1-\phi(\gamma_3))^2 \\ & - (1-\nu_0)N_b\phi(\gamma_2)\phi(\gamma_3)(1-\phi(\gamma_3)). \end{aligned} \quad (68)$$

Applying the same approach to the FAP at $\mathcal{SU}_{i_e}$, $i_e = 1, 2, \ldots, N_e$, in (25), we can easily prove that $P_{f,e}^{(\mathcal{SU})}$ is lower-bounded by

$$\begin{aligned}\bar{P}_{f,e}^{(\mathcal{SU})} =& 1 - (1 - (1-\nu_0)N_b\phi(\gamma_2)))(1-\phi(\gamma_3))^2 \\ & - (1-\nu_0)N_b\phi(\gamma_2)\phi(\gamma_3)(1-\phi(\gamma_3)) \end{aligned} \quad (69)$$

From (30), (68) and (69) with $\alpha = N_b/N$, $0 < \alpha \leqslant 1$, the average FAP of the HDTED scheme is lower-bounded by

$$\begin{aligned}\bar{P}_{f,l}^{(\mathcal{SU})} &= \frac{N_b\bar{P}_{f,b}^{(\mathcal{SU})} + N_e\bar{P}_{f,e}^{(\mathcal{SU})}}{N} \\ &= 1 - (1 - \alpha N\phi(\gamma_2)))(1-\phi(\gamma_3))^2 \\ &\quad - \alpha N\phi(\gamma_2)\phi(\gamma_3)(1-\phi(\gamma_3)). \end{aligned} \quad (70)$$

Appendix F
Proof of Lemma 9

As shown in Lemma 6, $\bar{P}_f^{(\mathcal{SU})} \geqslant \bar{P}_{f,l}^{(\mathcal{SU})}$. Thus, we have $\zeta_f \geqslant \bar{P}_{f,l}^{(\mathcal{SU})}$ since $\bar{P}_f^{(\mathcal{SU})} \leqslant \zeta_f$.

Finding α in (33) when $\bar{P}_{f,l}^{(\mathcal{SU})} = \zeta_f$, i.e.

$$\begin{aligned}& 1 - (1 - \alpha(1-\nu_0)N\phi(\gamma_2)))(1-\phi(\gamma_3))^2 \\ & - \alpha(1-\nu_0)N\phi(\gamma_2)\phi(\gamma_3)(1-\phi(\gamma_3)) = \zeta_f, \end{aligned} \quad (71)$$

we obtain the upper bound of α as

$$\alpha_u = \frac{\zeta_f + (1-\phi(\gamma_3))^2 - 1}{(1-\nu_0)N\phi(\gamma_2)(1-\phi(\gamma_3))(1-2\phi(\gamma_3)))}. \quad (72)$$

Note that $1 \geqslant \alpha_u > 0$ and $1/2 > \phi(x) > 0$, $\forall x > 0$. It can also be shown that $\phi(x)$ monotonically decreasing over x.

Therefore, in order to guarantee $\alpha_u > 0$, from (72), γ_3 should be greater than or equal to $\gamma_{3,l}$, which can be easily obtained as

$$\gamma_{3,l} = \phi^{-1}\left(1 - \sqrt{1-\zeta_f}\right). \quad (73)$$

References

[1] I. Mitola, J. and J. Maguire, G.Q., "Cognitive radio: Making software radios more personal," *IEEE Pers. Commun.*, vol. 6, no. 4, pp. 13–18, Aug. 1999.

[2] S. Haykin, "Cognitive radio: brain-empowered wireless communications," *IEEE J. Sel. Areas Commun.*, vol. 23, no. 2, pp. 201–220, Feb. 2005.

[3] A. Ghasemi and E. Sousa, "Spectrum sensing in cognitive radio networks: requirements, challenges and design trade-offs," *IEEE Commun. Mag.*, vol. 46, no. 4, pp. 32–39, 2008.

[4] T. Yucek and H. Arslan, "A survey of spectrum sensing algorithms for cognitive radio applications," *IEEE Commun. Surveys and Tutorials*, vol. 11, no. 1, pp. 116–130, first quarter 2009.

[5] D. Cabric, S. Mishra, and R. Brodersen, "Implementation issues in spectrum sensing for cognitive radios," in *Proc. ACSSC'04*, vol. 1, Pacific Grove, CA, USA, Nov. 2004, pp. 772–776.

[6] Z. Tian and G. B. Giannakis, "A wavelet approach to wideband spectrum sensing for cognitive radios," in *Proc. CROWNCOM'06*, Mykonos Island, Greece, Jun. 2006, pp. 1–5.

[7] Y. Zeng and Y.-C. Liang, "Covariance based signal detections for cognitive radio," in *Proc. IEEE DySPAN'07*, Dublin, Ireland, Apr. 2007, pp. 202–207.

[8] A. Sendonaris, E. Erkip, and B. Aazhang, "User cooperation diversity - Part I. System description," *IEEE Trans. Commun.*, vol. 51, no. 11, pp. 1927–1938, Nov. 2003.

[9] ——, "User cooperation diversity - Part II. Implementation aspects and performance analysis," *IEEE Trans. Commun.*, vol. 51, no. 11, pp. 1939–1948, Nov. 2003.

[10] J. Laneman, D. Tse, and G. Wornell, "Cooperative diversity in wireless networks: Efficient protocols and outage behavior," *IEEE Trans. Inf. Theory*, vol. 50, no. 12, pp. 3062–3080, Dec. 2004.

[11] K. Ben Letaief and W. Zhang, "Cooperative communications for cognitive radio networks," *Proc. of the IEEE*, vol. 97, no. 5, pp. 878–893, May 2009.

[12] G. Ganesan and Y. Li, "Cooperative spectrum sensing in cognitive radio, part I: Two user networks," *IEEE Trans. Wireless Commun.*, vol. 6, no. 6, pp. 2204–2213, Jun. 2007.

[13] T. Sanguanpuak and N. Rajatheva, "Performance analysis of primary user energy detection in a cognitive relay system with diversity," in *Proc. IEEE VTC 2011-Spring*, Budapest, Hungary, May 2011, pp. 1–5.

[14] W. Zhang and K. Letaief, "Cooperative spectrum sensing with transmit and relay diversity in cognitive radio networks," *IEEE Trans. Wireless Commun.*, vol. 7, no. 12, pp. 4761–4766, Dec. 2008.

[15] G. Xiong and S. Kishore, "Cooperative spectrum sensing with beamforming in cognitive radio networks," *IEEE Commun. Lett.*, vol. 15, no. 2, pp. 220–222, Feb. 2011.

[16] Q.-T. Vien, H. Tianfield, and B. G. Stewart, "Efficient cooperative spectrum sensing for cognitive wireless relay networks over Rayleigh flat fading channels," in *Proc. IEEE VTC 2012-Spring*, Yokohama, Japan, May 2012, pp. 1–5.

[17] S. Chaudhari, J. Lunden, V. Koivunen, and H. Poor, "Cooperative sensing with imperfect reporting channels: Hard decisions or soft decisions?" *IEEE Trans. Signal Process.*, vol. 60, no. 1, pp. 18–28, Jan. 2012.

[18] Y. Zou, Y.-D. Yao, and B. Zheng, "Cooperative relay techniques for cognitive radio systems: Spectrum sensing and secondary user transmissions," *IEEE Commun. Mag.*, vol. 50, no. 4, pp. 98–103, Apr. 2012.

[19] Q.-T. Vien, B. G. Stewart, H. Tianfield, and H. X. Nguyen, "Efficient cooperative spectrum sensing for three-hop cognitive wireless relay networks," *IET Commun.*, vol. 7, no. 2, pp. 119–127, 2013.

[20] W. Han, J. Li, Z. Li, J. Si, and Y. Zhang, "Efficient soft decision fusion rule in cooperative spectrum sensing," *IEEE Trans. Signal Process.*, vol. 61, no. 8, pp. 1931–1943, Apr. 2013.

[21] Q.-T. Vien, H. X. Nguyen, O. Gemikonakli, and B. Barn, "An efficient cooperative spectrum sensing under bandwidth constraint with user selection," in *Proc. IEEE VTC 2014-Fall*, Vancouver, Canada, Sep. 2014, pp. 1–5.

[22] Q.-T. Vien, H. X. Nguyen, R. Trestian, P. Shah, and O. Gemikonakli, "Performance analysis of cooperative spectrum sensing for cognitive wireless radio networks over Nakagami-m fading channels," in *Proc. IEEE PIMRC 2014*, Washington, DC, USA, Sep. 2014, pp. 738–742.

[23] Q.-T. Vien, H. X. Nguyen, L.-N. Tran, and E.-K. Hong, "Double-threshold based cooperative spectrum sensing over imperfect channels," in *Proc. IEEE WCNC 2015*, New Orleans, Louisiana, USA, Mar. 2015, pp. 293–298.

[24] C. Sun, W. Zhang, and K. Letaief, "Cooperative spectrum sensing for cognitive radios under bandwidth constraints," in *Proc. IEEE WCNC'07*, Hong Kong, 2007, pp. 1–5.
[25] J. Wu, T. Luo, J. Li, and G. Yue, "A cooperative double-threshold energy detection algorithm in cognitive radio systems," in *Proc. WiCOM'09*, Beijing, China, 2009, pp. 1–4.
[26] H. Vu-Van and I. Koo, "Cooperative spectrum sensing with double adaptive energy thresholds and relaying users in cognitive radio," in *Proc. AICT'10*, Barcelona, Spain, May 2010, pp. 52–56.
[27] S.-Q. Liu, B.-J. Hu, and X.-Y. Wang, "Hierarchical cooperative spectrum sensing based on double thresholds energy detection," *IEEE Commun. Lett.*, vol. 16, no. 7, pp. 1096–1099, 2012.
[28] J. Jafarian and K. A. Hamdi, "Non-cooperative double-threshold sensing scheme: A sensing-throughput tradeoff," in *Proc. IEEE WCNC 2013*, Shanghai, China, 2013, pp. 3376–3381.
[29] T. E. Bogale, L. Vandendorpe, and L. B. Le, "Sensing throughput tradeoff for cognitive radio networks with noise variance uncertainty," in *Proc. CROWNCOM 2014*, Oulu, Finland, Jun. 2014.
[30] A. Ghasemi and E. S. Sousa, "Opportunistic spectrum access in fading channels through collaborative sensing," *J. Commun.*, vol. 2, no. 2, pp. 71–82, Mar. 2007.
[31] F. F. Digham, M.-S. Alouini, and M. K. Simon, "On the energy detection of unknown signals over fading channels," *IEEE Trans. Commun.*, vol. 55, no. 1, pp. 21–24, Jan. 2007.
[32] I. S. Gradshteyn and I. M. Ryzhik, *Table of Integrals, Series, and Products*, 7th ed. Academic Press, 2007.
[33] S. Stotas and A. Nallanathan, "Optimal sensing time and power allocation in multiband cognitive radio networks," *IEEE Trans. Commun.*, vol. 59, no. 1, pp. 226–235, Jan. 2011.
[34] M. K. Simon and M.-S. Alouini, *Digital Communication over Fading Channels*, 2nd ed. John Wiley & Sons, 2005.

Quoc-Tuan Vien (S'10, M'12) received his B.Sc. degree from Ho Chi Minh City University of Technology, Vietnam, in 2005; his M.Sc. degree from Kyung Hee University, South Korea, in 2009; and his Ph.D. degree from Glasgow Caledonian University, U.K., in 2012, all in telecommunications.

From 2005 to 2007, he was with Fujikura Fiber Optics Vietnam Company as a Production-System Engineer. From 2010 to 2012, he worked as a Research and Teaching Assistant at Glasgow Caledonian University. In Spring 2013, he worked as Postdoctoral Research Assistant at Nottingham Trent University, U.K. He is currently a Lecturer with the School of Science and Technology, Middlesex University, London, U.K. His research interests include MIMO, space-time coding, network coding, physical layer security, cross-layer design and optimisation, relay networks, cognitive radio networks, heterogeneous networks, and cloud radio access networks. Dr. Vien is a Member of the IEEE, IEEE Young Professionals, and the IET.

Huan X. Nguyen (M'06, SM'15) received his B.Sc. in Electronics and Telecommunications from Hanoi University of Science and Technology in 2000, and his Ph.D. in Electrical Engineering from the University of New South Wales, Australia, in 2006. In 2007, he joined the Institute of Advanced Telecommunications (IAT) at Swansea University as a Research Officer. From 2008 to 2010, he was a Lecturer at the School of Engineering and Computing, Glasgow Caledonian University, U.K. He joined the School of Science & Technology, Middlesex University, U.K., as a Senior Lecturer in 2011. His research interests include PHY security, multiple input multiple output (MIMO) techniques, LTE systems, relay and cognitive networks. Dr. Nguyen is a Senior Member of the IEEE.

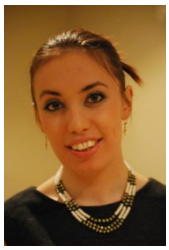

Ramona Trestian (S'08, M'12) is a Senior Lecturer with the Design Engineering and Mathematics Department, School of Science and Technology, Middlesex University, London, U.K. She received her Ph.D. degree from Dublin City University, Ireland, in 2012. Prior to joining Middlesex University, she worked with IBM Research Dublin as an IBM/IRCSET Exascale Postdoctoral Researcher. She has published in prestigious international conferences and journals and has two edited books. She is a reviewer for international journals and conferences. Her research interests include mobile and wireless communications, user perceived quality of experience, multimedia streaming, handover and network selection strategies, and software-defined networks. Dr. Trestian is a member of the IEEE, IEEE Young Professionals, IEEE Communications Society, and IEEE Broadcast Technology Society.

Purav Shah (S'05, M'09) is a Senior Lecturer in the Design, Engineering and Mathematics Department at Middlesex University London. He received his Ph.D. in Communication and Electronics Engineering from University of Plymouth, U.K., in 2008. He worked as an Associate Research Fellow at the University of Exeter on EU-FP6 PROTEM project on scanning probe-based memories from 2008 to 2010. His work included read channel design; noise modelling and signal processing for probe storage. His research interests broadly are in the field of performance evaluation of wireless sensor networks (protocols, routing, and energy efficiency), Internet of Things (IoT) and M2M solutions, system modelling of heterogeneous wireless networks, Intelligent Transportation Systems (ITS) and Big Data Analysis of network traffic. He is an active member of the IEEE (MIEEE) and a reviewer of the IET Electronics Letters, IEEE Transactions on Circuits and Systems for Video Coding, KSII Transactions on Internet and Information Systems, MDPI Sensors and International Journal on Communication Systems (IJCS), Wiley.

Orhan Gemikonakli obtained his first degree in electrical engineering from Eastern Mediterranean University in Cyprus, in 1984. He then continued his studies at King's College, University of London where he obtained his M.Sc. in Digital Electronics, Computers and Communications, and Ph.D. in Telecommunications in 1985 and 1990 respectively. He worked there as a post-doctoral Research Associate for a couple of years before moving in 1990 to Middlesex University, London where he is now a research professor, and a senior manager leading the School's international activities. He is a member of the IET and a Chartered Engineer. His research interest is in telecommunications, network security, and performability modelling of complex systems. Prof. Gemikonakli published more than 100 research papers in refereed journals and conference proceedings. He serves on various Conference Programme Committees and Editorial Boards. His e-mail address is: o.gemikonakli@mdx.ac.uk and his Web-page can be found at http://www.mdx.ac.uk/about-us/our-people/staff-directory/gemikonakli-orhan